The scope of the Basin Inspection / Monitoring Activities involves;

a) Triennial monitoring of ground water for chemical species that can deteriorate the basin and filter structure inaccessible concrete[GB(Pc2].
b) Annual visual broad inspections of exposed concrete and building structures housing spent fuel.
c) 5-year visual inspections by qualified inspectors of exposed concrete and building structures
d) Visual inspection of normally inaccessible components of the fuel storage system in the event a basket is lifted in preparation for movement.
e) Continuous monitoring of the leak detection sump level

Visual inspections identify physical degradation of the exposed surfaces of the concrete structures. Qualified inspectors examine the fuel storage basin concrete, building structure and liner at 5-year intervals relative to the requirements of ACI 349.3R. These examinations are supplemented with annual inspections by operations staff for deterioration of the concrete due to loss of material, cracking or spalling, and steel building structures due to corrosion and coating degeneration. A visual inspection of normally inaccessible components in the basin, baskets, grid, basin liner, if/when they are moved will identify degradation of the material resulting from corrosion. Inspections provide reasonable assurance that any degradation of the fuel storage system is identified.

Monitoring and Trending – All SSCs covered by the Structures Monitoring AMP are non-safety related as defined in 10CFR50.65. These structures have been ranked based on risk significance and are monitored based on condition. Results from condition monitoring activities are analyzed against predetermined goals annually in accordance with SOP 16-17. Deficiencies are corrected commensurate with the associated safety significance and may necessitate adjustments to monitoring frequency and/or implementation of trending for structures with high risk significance.

The basin leak detection system continuously monitors the sump level via the Site Instrumentation Monitoring System (SIMS) and constantly displays the level on a monitoring screen. Alarms are triggered if the level exceeds pre-set values.

The eight NRC reviewed and approved ground water sampling wells at MO are used to monitor for any potential leakage of basin water to the surrounding soil. The wells are sampled routinely per SOP 16-102, Sample Well Analysis Compliance Test. In addition, at least 1 of 3 of the wells positioned around the basin are used to monitor ground water for potential effects on below grade concrete.

Acceptance Criteria - Table 2 summarizes acceptance criteria based on the type of inspection and the associated structure.

Corrective Actions - Visual inspection acceptance criteria are based on the absence of indications that are signs of degradation. Engineering evaluations determine whether observed deterioration of material condition is significant enough to compromise the ability of the SSC to perform its intended function. Occurrence of degradation that is adverse to quality will be entered into the Corrective Action System. Alarm panel response procedures identify the various criteria for the different fuel storage system monitoring devices at GEH-MO and specify any required corrective actions and responses.

Confirmation Process - The process of confirmation is controlled by the Morris quality program and is consistent with the requirements of 10CFR72, Subpart G.

Administrative Controls – Administrative controls are governed by the Morris quality program. This program implements controls that are consistent with the requirements of 10CFR72, Subpart G.

Operating / Industry Experience - A review of the results of SOP 16-17, Fuel Storage System Inspection, indicates that although there is some degradation visible in some of the painted structures, there is no visible evidence that the concrete or stainless steel structures that are accessible for inspection are degrading/degraded to any extent that would indicate their functionality has in any way changed over the review period. The inspections have been conducted by veteran operators, one of which has been employed at MO for over 40 years. Minor paint issues are addressed as they are observed and due to the humid conditions in the area of the fuel pools, these minor issues are to be expected.

Regulatory information presented in NUREG-1522 and NUREG/CR-6927 was also reviewed to ensure degradation parameters selected for the identified structures were consistent with the published findings. This review concluded that the aging mechanisms described in NUREG-1801 for fuel storage facilities do indeed cover the concrete and steel deteriorations noted in NUREG-1522 and NUREG/CR-6927. It should also be noted that the concrete structures at GEH-MO were designed and constructed in accordance with the applicable national standards, specifically ACI 318-63, and meet conditions consistent with longevity as described by the Gall Report.

WATER CHEMISTRY AMP

As identified in Table 1, SSCs constructed from stainless steel, and necessitating maintenance of water chemistry, are maintained according to this Water Chemistry AMP. AMP elements are consistent with those in XI.M2 from NUREG 1801 Rev. 2 and are as follows:

Scope –Maintenance of water chemistry in contact with stainless steel SSCs ensures there is no material loss that would affect the functionality of structures important to safety. This is facilitated by water replenishing / filtering systems in combination with periodic monitoring in

accordance with this AMP. The stainless steel SSCs identified during the AMR that are managed with this AMP are denoted as "Water Chemistry" in Table 1.

Preventative Actions – This AMP involves SOPs that specify limits for the total amount of radioactivity and conductivity in the fuel basin water, sampling and analysis frequencies, and corrective actions for control of water chemistry. Fuel Basin water chemistry is controlled to minimize contaminant concentration thereby mitigating loss of material due to general, crevice, and pitting corrosion and cracking caused by SCC. Water chemistry is maintained within approved license specifications through continuous filtration and addition of ultra-pure water (typically 0.056 μmho/cm) as needed to maintain basin level.

Parameters Monitored / Inspected – Gross Beta and Conductivity

Detection of Aging Effects – Aging is mitigated by maintenance of basin water for structures in Table 1 involving stainless steel by:

a) Continued analysis of fuel storage basin water quality in accordance with a Compliance Test insuring conformity to license specifications.
b) Monthly sample analysis of water from the Basins using an independent lab.

Monitoring and Trending – Basin water radioactivity and conductivity is periodically recorded, evaluated and trended in accordance with SOP 16-10.

Acceptance Criteria – Basin water has the following radioactivity and conductivity limits:

a) Conductivity must be <1.35 μMho/cm.
b) Basin water activity (gross beta) must be less than 0.02 μCi/ml

Corrective Actions – Non-compliant samples indicating conditions adverse to quality will be entered into the Corrective Action System. Alarm panel response procedures identify the various criteria for the different fuel storage system monitoring devices at GEH-MO and specify any required corrective actions and responses.

Confirmation Process – The process of confirmation is controlled by the Morris quality program and is consistent with the requirements of 10 CFR 72 Part G.

Administrative Controls – Administrative controls are governed by the Morris quality program. This program implements controls that are consistent with the requirements of 10 CFR 72 Part G.

Operating Experience - All SSC's in the basin are 304 Stainless Steel. Per IAEA-TECDOC-1012, "Durability of Spent Nuclear Fuels and Facility Components in Wet Storage", SS wet storage facility components have excellent histories of durability in periods approaching 40

years provided that good water chemistry control is maintained. The GE-MO basin water chemistry provides an excellent media for SS materials. Combining the basin liner coupon examination, and the guidance from the IAEA Report, corrosion is minimal and should have little or no impact on the basin liner or other stainless-steel components of the fuel storage (baskets and supporting grid) system for the term of the license renewal. In addition, all of these components have been in a static mode since the last fuel receipt in January 1989, so there also hasn't been any mechanical wear.

As shown in GE-MO 72.48 prepared February 16, 1996, conductivity is a more accurate way to measure ultra-pure water quality than pH and a conductivity value of 2.5 µmho/cm was established, corresponding to a pH of 4.5 to 9.0 in keeping with the reference license specification. The 2004 GE-MO 72.48 lowers that value to 1.35 µmho/cm for the basin water, equivalent to a pH value of 5.5 to 8.0. This change is in keeping with the requirements in NUREG 1801, Chapter III establishing a lower limit of 5.5 pH for water as non-aggressive to concrete or stainless steel. This value is also representative of the typical GE-MO basin water quality. Since March 1976 the average basin water conductivity has been 1.07 µmho/cm. There are no sources for NaNo3 and Cl in the basin environment and values for these materials repeatedly are below detectable limit. During a recent test, basin water makeup, cooling and filtration were discontinued for a period of 50 days resulting in an actual conductivity increase to 1.22 µmho/cm. A conductivity value of 1.35 µmho/cm also provides a much lower tolerance for ionic impurities allowing the elimination of NaNo3 and Cl measurements since values well below 5 ppm of either cause conductivity to significantly increase beyond 1.35 µmho/cm.

ANCILLARY EQUIPMENT IMPORTANT TO SAFETY

All cranes are maintained in compliance with the requirements specified in 10 CFR 1910.179 (OSHA) and tracked by our Preventive Maintenance (PM) program described in MOI 401. The cranes are inspected, and routine maintenance items performed quarterly by on-site Maintenance personnel per the manufacturers recommended schedule. Annually, an independent inspection company performs a complete inspection, including non-destructive testing, of all cranes and hoists on site.

All grapples and miscellaneous tooling used for moving fuel bundles or fuel baskets are laid away. Each tool will undergo thorough inspection and testing to insure it complies with the original manufacturers specifications prior to utilizing it for lifting any fuel bundle or basket. When in use, these tools are only exposed to treated water described in the Water Chemistry AMP.

FUEL BASIN LINER TLAAs

In June 1993, the fuel storage basin was inspected to confirm expectations of continued structural integrity, as well as confirm the absence of microbe-induced corrosion (MIC). To confirm and document the integrity of the liner, a routine inspection plan was developed in

accordance with ASME Boiler and Pressure Vessel Code and other industry approved IVVI procedures. The inspection plan included use of underwater TV cameras to inspect the basin welds.

The results of this inspection showed, that based on high-resolution visual inspection and surface examination, the basin liner is judged to have continued integrity, with no environmental degradation associated with 20+ years of fuel storage. Also, considering the continuous maintenance of high purity water flow in the fuel storage basins continued long-term service is indicated.

The above is detailed in report GENE 689-013-0893, "Morris Fuel Recovery Center Fuel Storage Basin Liner Visual Examination Summary Report", dated September 1993.

Additionally, in 1994 an approximately 1.5" x 3.5" coupon was cut from the basin liner in the cask unloading pit. This area then had a patch welded over it. The sample was sectioned for optical metallography and scanning electron microscopy (SEM). Cross sectional views did not find evidence of significant surface attack, and the maximum surface penetration was 0.4 mils. SEM examination of the surface found oxide deposits, which is expected for a stainless steel that has been exposed to a water environment for 20+ years. Chemical analysis of the deposits determined the composition to be mostly iron oxide. No detrimental chemical species were found. No evidence of MIC phenomena was observed.

The nominal liner wall thickness in the unloading pit is 0.125 inches. Assuming the degradation occurred over 20 years and the corrosion rate remained constant, the liner would not be penetrated for the foreseeable future.

See report number GENE-689-003-0494, "Morris Fuel Recovery Center Fuel Storage Basin Liner Metallurgical Evaluation"; dated May 1994.

FUEL BUNDLE STORAGE

In broad, generic terms, the design and operation of the GEH-MO spent fuel pool is similar to a spent fuel storage pool at a nuclear power plant and some aspects of the reference NUREGs may be applicable, however, significant differences between GEH-MO basins and support systems and a nuclear power plants fuel storage basins and the fuel stored in both must also be taken into account. The GE-MO basins are below ground, in native bedrock, water level is maintained at or below grade level. All stored fuel is held in GEH-MO unique stainless-steel baskets (CSAR Section 5.0, ¶ 5.4.4.2) that are a "can" style container minus a lid, providing individual support and additional containment and shielding for each fuel bundle. Fuel is not routinely shuffled nor is new fuel added unlike the spent fuel pool in a nuclear power plant, (last fuel moved was January 1989) and there are no plans to do so. The static state of the GEH-MO fuel assures there are no mechanical or dynamic stresses placed on the fuel. The large basin water volume and low decay heat input from the stored fuel provide an extended period of time

to take corrective action in case of a malfunction of any of the basin support systems. In the event of an earthquake or other extreme natural phenomena, sufficient makeup water is available through either on-site or off-site means to maintain safe storage conditions.

Fuel stored at GEH-MO has reactor discharge dates that range from April 1970 through October 1986. The last fuel was received at GEH-MO in January 1989. Burnup rates range from a high of 36.71 GWD/MTU to a low of 0.18 GWD/MTU, and an average burnup of 17.74 GWD/MTU. Due to the robust design of the pool (CSAR Section 5.0, ¶ 5.5) and the time interval from reactor discharge, there are no postulated events that would result in exposure to a member of the public in excess of the limits of 10CFR72.104, as stated in the CSAR, Section 8.0, ¶ 8.1.1. The condition of the fuel is monitored as part of routine activities conducted at GEH-MO through basin water analysis and air quality monitoring. The design of the pool, and operational requirements for the basin area assure a depth of water over the stored fuel, which provides for extended passive heat dissipation capability. In May of 2004, a test was performed in to demonstrate the water quality would be minimally affected if there were a total loss of the Basin cooling and filtration systems. Results of the test revealed the conductivity approached 1.24μmho/cm, well below the license specification. Also demonstrated in the test was that heat dissipation from the basin was adequate as the basin water temperature reached a mere 123°F. Basin water level decreased to the 46' 9" el., 9' 6'' above the upper most portion of the fuel bundle, leaving an additional 6" before reaching the license limit of 9' above the upper most part of the fuel bundle.

In general, safe storage of the spent fuel is achieved by maintaining the integrity of the fuel cladding through maintaining a high quality of basin water (CSAR Section 10.0, ¶ 10.4.5) and substantiated by IAEA-TECDOC-1012, "Durability of Spent Nuclear Fuels and Facility Components in Wet Storage". Fuel cladding is designed to withstand a far more severe environment in a reactor than in static storage at GEH-MO. The low temperature conditions, removal of both particulate and ionized impurities from the basin water, and absence of chemical materials provides high water clarity, limits corrosion and maintains radiation exposure rates in the vicinity of the basin as low as reasonably achievable. The cladding provides an effective primary barrier to the escape of fission or activation products from stored fuel. The basin water is an effective secondary barrier for the confinement of the small amounts of radioactive materials that may be released from the spent fuel.

The GEH-MO radiation protection program is previously established in the current approved revision of the GEH-MO Consolidated Safety Analysis Report (CSAR) Section 7.0, Radiation Protection. Subsection 7.7, Estimated Man-Rem Off Site Dose Assessment, specifies the current approved environmental monitoring program. Under normal operating conditions, Kr-85 provides essentially all the exposure from the GEH-MO ventilation exhaust stack. The sum of the values for annual whole-body exposure due to inhalation and skin dose out to a radius of 50 miles gives a total of less than 2×10^{-6} man-Rem/yr whole body and less than 0.12 man-Rem skin dose. Routine air samples continue to show that exhaust emissions are below detectable limit, as follows:

Vent Supply	Stack Inlet	
Alpha (µCi/ml)	3.0×10^{-13}	MDA (~3×10^{-15})
Beta (µCi/ml)	6.0×10^{-13}	MDA (~3×10^{-15})

The vent supply is air intake to the facility and stack inlet is air being released to the exhaust stack.

There are no planned or unplanned releases of liquid wastes from the site boundaries.

Analysis of postulated accidents including the causes of such events, consequences, and the ability of GEH-MO to cope with each are previously established in the CSAR, Section 8.0, Accident Safety Analysis. The Structures, Systems, and Components (SSCs) Important to Safety are described in Section 11.0, Quality Assurance. Both have been in the CSAR since the original Part 50 license, SNM-1265 was issued for GEH-MO and were included during the 1979 license renewal application and subsequent issue of the current Part 72 license SNM-2500 in 1982. As such, both are considered part of the original licensing basis for Morris Operation. Given the robust design of the Morris pool and the passive nature of the SSCs Important to Safety, no scenario involving a support system would result in an exposure to the public in excess of the criteria established in 10CRF72.104.

The current approved safety basis for the Morris facility as defined in the CSAR, designated items important to safety (CSAR Section 11.0, sub-section 11.3) demonstrates that no accident postulated (CSAR Section 8.0) will result in exceeding the limits of 10 CFR 72.104 and 10 CFR 100.20 to demonstrate protection of the public.

As shown in CSAR Sections 7.0 and 8.0, the low value of credible doses which could be received from normal operating and credible accident releases are many orders of magnitude below regulatory limits.

Unlike similar support systems at a nuclear power plant, the combination of the GEH-MO radiation safety program, accident analysis and functional classification of equipment demonstrates that failure of a SSC supporting fuel storage basin operation will not cause an immediately reportable event. Ample time has been demonstrated for repair, temporary substitution, or permanent replacement of any SSC to prevent any Technical Specification violation and without exceeding any regulatory limits for radiation exposure is postulated.

Summary

Based on the reference information supplied in IAEA-TECDOC-1012, "Durability of Spent Nuclear Fuels and Facility Components in Wet Storage", and NUREG 1801, "Generic Aging Lessons Learned (GALL) Report", the effects of aging are minimal and will be adequately

managed for the duration of the license period through the GE-MO Aging Management Program.

Aging Management Program Review
Table 1

III STRUCTURES AND COMPONENT SUPPORTS
A5 Group 5 Structures (Fuel Storage Facility, Refueling Canal)

Item	Link	Structure and/or Component	Material	Environment	Aging Effect / Mechanism	Aging Management Program (AMP)	Further Evaluation
II.A5.TP-25	III.A5-2 (T-03)	FSB/FCS Concrete (accessible areas): all	Concrete	Any environment	Cracking due to expansion from reaction with aggregates	"Structures Monitoring"	No
III.A5.TP-27	III.A5-4(T-05)	FSB/FCS Concrete (accessible areas): below-grade exterior; foundation	Concrete	Ground water/soil	Cracking; loss of bond; and loss of material (spalling, scaling) due to corrosion of embedded steel	"Structures Monitoring"	No
III.A5.TP-23	III.A5-6(T-01)	FSB/FCS Concrete (accessible areas): exterior above- and below-grade; foundation	Concrete	Air – outdoor	Loss of material (spalling, scaling) and cracking due to freeze-thaw	"Structures Monitoring"	No
III.A5.TP-24	III.A5-7(T-02)	FSB/FCS Concrete (accessible areas): exterior above- and below-grade; foundation	Concrete	Water – flowing	Increase in porosity and permeability; loss of strength due to leaching of calcium hydroxide and carbonation	"Structures Monitoring"	No
III.A5.TP-26	III.A5-9(T-04)	FSB/FCS Concrete (accessible areas): interior	Concrete	Air – indoor, uncontrolled or Air – outdoor	Cracking; loss of bond; and loss of material (spalling, scaling)	"Structures Monitoring"	No

		and above-grade exterior			due to corrosion of embedded steel		

Item	Link	Structure and/or Component	Material	Environment	Aging Effect / Mechanism	Aging Management Program (AMP)	Further Evaluation
III.A5.TP-204	III.A5-2(T-03)	FSB/FCS Concrete (inaccessible areas): all	Concrete	Any environment	Cracking due to expansion from reaction with aggregates	The concrete structures at GEH-MO were designed and constructed in accordance with ACI 318-63 and meet conditions for longevity as described by the Gall Report. Aggregates per ACI 318-63 conform with ASTM C33 "Specifications for Concrete Aggregates" as referenced by ASTM C295.	No
III.A5.TP-212	III.A5-4(T-05)	FSB/FCS Concrete (inaccessible areas): below-grade exterior; foundation	Concrete	Ground water/soil	Cracking; loss of bond; and loss of material (spalling, scaling) due to corrosion of embedded steel	"Structures Monitoring"	No
III.A5.TP-29	III.A5-5(T-07)	FSB/FCS Concrete (inaccessible areas): below-grade exterior; foundation	Concrete	Ground water/soil	Increase in porosity and permeability; cracking; loss of material (spalling, scaling)	"Structures Monitoring"	No
III.A5.TP-67	III.A5-7(T-02)	FSB/FCS Concrete (inaccessible areas): exterior	Concrete	Water – flowing	Increase in porosity and permeability; loss of strength	N/A - There are no exterior GEH-MO concrete structures in contact with untreated flowing water.	N/A

		above- and below-grade; foundation			due to leaching of calcium hydroxide and carbonation		

Item	Link	Structure and/or Component	Material	Environment	Aging Effect / Mechanism	Aging Management Program (AMP)	Further Evaluation
III.A5.TP-108	III.A5-6(T-01)	FSB/FCS Concrete (inaccessible areas): foundation	Concrete	Air – outdoor	Loss of material (spalling, scaling) and cracking due to freeze-thaw	N/A. There are no GEH-MO inaccessible areas are subject to outdoor air.	N/A
III.A5.TP-114	III.A5-1(T-10)	FSB/FCS Concrete: all	Concrete	Air – indoor, uncontrolled	Reduction of strength and modulus due to elevated temperature (>150°F general; >200°F local)	N/A. There are no GEH-MO concrete structures subject to temperatures above 150°F	N/A
III.A5.TP-30	III.A5-3(T-08)	FSB/FCS Concrete: all	Concrete	Soil	Cracking and distortion due to increased stress levels from settlement	"Structures Monitoring" GEH-MO does not have a de-watering system.	No
III.A5.TP-31	III.A5-8(T-09)	FSB/FCS Concrete: foundation; subfoundation	Concrete; porous concrete	Water – flowing under foundation	Reduction of foundation strength and cracking due to differential settlement and erosion of porous concrete subfoundation	"Structures Monitoring" GEH-MO does not have a de-watering system.	No

III.A5.TP-28	III.A5-10(T-06)	FSB/FCS Concrete: interior; above-grade exterior	Concrete	Air – indoor, uncontrolled or Air – outdoor	Increase in porosity and permeability; cracking; loss of material (spalling, scaling) due to aggressive chemical attack	"Structures Monitoring"	No

Item	Link	Structure and/or Component	Material	Environment	Aging Effect / Mechanism	Aging Management Program (AMP)	Further Evaluation
II.A5.TP-300		High-strength structural bolting	Low-alloy steel, actual measured yield strength ≥ 150 ksi	Air – indoor, uncontrolled or Air – outdoor	Cracking due to stress corrosion cracking	N/A. There are no GEH-MO structures secured with High-strength (≥ 150 ksi) bolts.	N/A
III.A5.T-12	III.A5-11(T-12)	Masonry walls: all	Concrete block	Air – indoor, uncontrolled or Air – outdoor	Cracking due to restraint shrinkage, creep, and aggressive environment	N/A. There are no masonry structures at GEH-MO.	N/A
III.A5.TP-34		Masonry walls: all	Concrete block	Air – outdoor	Loss of material (spalling, scaling) and cracking due to freeze-thaw	N/A. There are no masonry structures at GEH-MO.	N/A
III.A5.TP-302	III.A5-12(T-11)	FSB Building Steel components: all structural steel	Steel	Air – indoor, uncontrolled or Air – outdoor	Loss of material due to corrosion	"Structures Monitoring"	No
III.A5.T-14	III.A5-13(T-14)	FSB S-Steel components: fuel pool liner, Grapples, Doorway Guard, Expansion Gate, Fuel Cladding	Stainless steel	Treated water or Treated borated water	Cracking due to stress corrosion cracking; Loss of material due to pitting and crevice corrosion	"Water Chemistry" and "Structures Monitoring" Additionally, spent fuel pool water level is maintained in accordance with SOP 1-10 technical specifications and leakage from the leak chase channels is monitored in accordance with SOP 1-27. TLAAs involving IVVI inspections and liner coupon extractions provide additional	No, unless leakages have been detected through the SFP liner that cannot be accounted for from the leak chase channels

						support that water chemistry control is effective at managing aging effects.	

Item	Link	Structure and/or Component	Material	Environment	Aging Effect / Mechanism	Aging Management Program (AMP)	Further Evaluation
III.A5.TP-261		FSB Building Structural bolting	Any	Any environment	Loss of preload due to self-loosening	"Structures Monitoring"	No
III.A5.TP-248		FSB Building Structural bolting	Steel	Air – indoor, uncontrolled	Loss of material due to general, pitting and crevice corrosion	"Structures Monitoring"	No
III.A5.TP-274		FSB Building Structural bolting	Steel; galvanized steel	Air – outdoor	Loss of material due to general, pitting, and crevice corrosion	"Structures Monitoring"	No

Structures Monitoring
Table 2 – Acceptance Criteria

Concrete Surfaces	Concrete Embedments	Steel Structures	Stainless Steel Liner (with Leak Detection)
Absence of leaching and chemical attack	Concrete surface condition attributes are met	Loss or degraded areas of coatings less than or equal to 4,000 mm^2 (6 $in.^2$) at one area	No increase in leakage rate observed in leak-detection system
Absence of abrasion, erosion, and cavitation	Absence of corrosion of the exposed embedded metal surfaces and corrosion stains around the embedded metal	Loss or degraded areas of coatings less than or equal to 10,000 mm^2 (16 $in.^2$) over the gross surface of the structure	Absence of bulges or depressions in liner plate – related to aging not construction
Popouts and voids less than 20 mm (3/4 in.) in diameter or equivalent surface area	Absence of detached embedments or loose bolts		Basin Water Analysis: - Gross beta < 0.02 µCi/ml - Conductivity <1.35 µMho/cm.
Scaling less than 5 mm (3/16 in.) in depth	Absence of indications of degradation due to vibratory loads from piping and equipment		
Spalling less than 10 mm (3/8 in.) in depth and 100 mm (4 in.) in any dimension			
Absence of any signs of corrosion in the steel reinforcement or anchorage components			
Passive cracks less than 0.4 mm (0.015 in.) in maximum width (note 1)			
Absence of excessive deflections, settlements, or other physical movements that can affect structural performance			
Monitoring Well Analysis (at least 1 of 3): - Verification of non-aggressive ground water or soil			

(pH > 5.5, chlorides < 500 ppm, or sulfates <1500 ppm)			
Notes: 1. passive cracks are defined as those having and absence of recent growth and an absence of other degradation mechanisms at the crack			

A.9 FUEL STORAGE SYSTEM HEAT TRANSFER

A.9.1 INTRODUCTION

In 2004 a physical test was performed in the GE Hitachi Morris Operation (GEH-MO) Fuel Basins to determine how long the Basin Water could perform its safety function without the aid of any support systems operating, and devoid of any License Specification infractions.

A.9.2 Initial Conditions

Prior to commencing the test, baseline temperature and conductivity readings were taken at various locations in both fuel basins, transfer isle and unloading pit (see attached fuel basin map). Data was also recorded at three different elevations in each of those locations.

Elevation[1] (feet)	45	35	25	5
Distance above basin/transfer isle floor	23' 6"	13' 6"	3' 6"	n/a
Distance above unloading pit floor	45'	Not recorded	25'	5'

[1] Zero (0) foot elevation corresponds to the bottom of the unloading pit.

The initial readings revealed consistent results of equal temperature and similar conductivity at all locations where data was taken. This indicates there is uniform mixing of basin water in all locations. Numerically, the initial basin water temperature was 77°F with a mean conductivity reading of 1.06 ±0.05μmho/cm.

The basin support systems, utilized to maintain basin water temperature and water quality, were shut down. Specifically, both basin evaporator chiller units and their respective chiller (circulation) pumps and the basin filter system.

The Basin Leak detection system was left in operation so it could be monitored independently of the ongoing basin study. To better simulate loss of all support systems the basin leak detection system pump-out was realigned to a holding tank.

To guarantee there would be no violation of any license requirements, one of the plant ventilation exhaust blowers was left in operation to insure there was positive air flow through the sand filter and out the stack.

A.9.3 Evaluation

For the purpose of this evaluation, figures have been provided depicting the elevations of components within the fuel basin and the locations where conductivity and temperature measurements were taken.

Additionally, provided information includes: bar graphs depicting basin conductivity, level and temperature for the basin water at the beginning of the test and the last day of the test, as well as line graphs depicting same information for entire duration of test.

A.9.3.1 Fuel Basin Conductivity

For comparative purposes, all the conductivity readings for all locations were averaged to get the mean conductivity for each day. The greatest variance observed between all locations where data was taken was only 0.02µmho/cm.

As basin water temperature increased conductivity decreased (from 1.06µmho/cm) at an average rate of 0.013µmho/cm per day for the first nineteen days down to 0.81µmho/cm. For the next twenty-one days, conductivity increased at an average rate of 0.012µmho/cm per day. During the final ten days of the test slightly less than a 0.02µmho/cm per day increase in conductivity was observed. The highest conductivity (1.23µmho/cm) was measured on the forty-ninth day, the day before the conclusion of the test. The average conductivity at the conclusion of the test, day fifty, was 1.22µmho/cm.

A.9.3.2 Fuel Basin Level (See Figure 1 depicting various basin elevations)

At the start of the test, Basin level was recorded to be at the 50'el. which is the normal operating level of the basin water. Level decreased about 0.1"/day for the first 6 days. The next 9 days increased in even increments until the level was decreasing almost an inch a day. Level continued decreasing slightly less than an inch per day for the next 16 days. For the final 19 days, basin level decreased slightly more than an inch per day. At the end of fifty days the final basin water level was at the 46' 9" elevation mark having dropped a total of 3' 3". The final level was still more than six inches above the licensing requirement that the basin level cannot be less than 9' above the upper most portion of the fuel bundle.

A.9.3.3 Fuel Basin Temperature

Normal basin water temperature is maintained at 77°F±2° and basin temperature was 77°F at the start of the test. During the first seven days, basin temperature increased at the rate of three degrees a day. The next twelve days temperature in rose on the average of slightly over one degree per day, followed by twenty one days where temperature was increasing a little less than

one-half (0.5) degree daily. For the final ten days of the test there was no temperature change and the basin remained at a constant 123°F.

A.9.4 Summary

A review of the data presented proves the GEH-MO Fuel Storage Basins can fulfill their intended function of maintaining water conductivity and level without violation of any license specifications for a minimum of fifty days without any support system in operation.

An important point to emphasize here is that basin temperature and conductivity readings, without any support systems operating, were fairly consistent at all locations in the basin for a particular day, throughout the entire testing period. This proves that there is a constant natural circulation of basin water and all equipment in the basin is exposed to water of the same quality and temperature.

The results also illustrate there is still a comfortable margin past the fifty day mark, upwards to an additional ten days, before the basin water level would reach the license specification elevation of 46' 3".

Figure 1
Basin Water Elevations
for Condutivity Test
May–Jun 2004

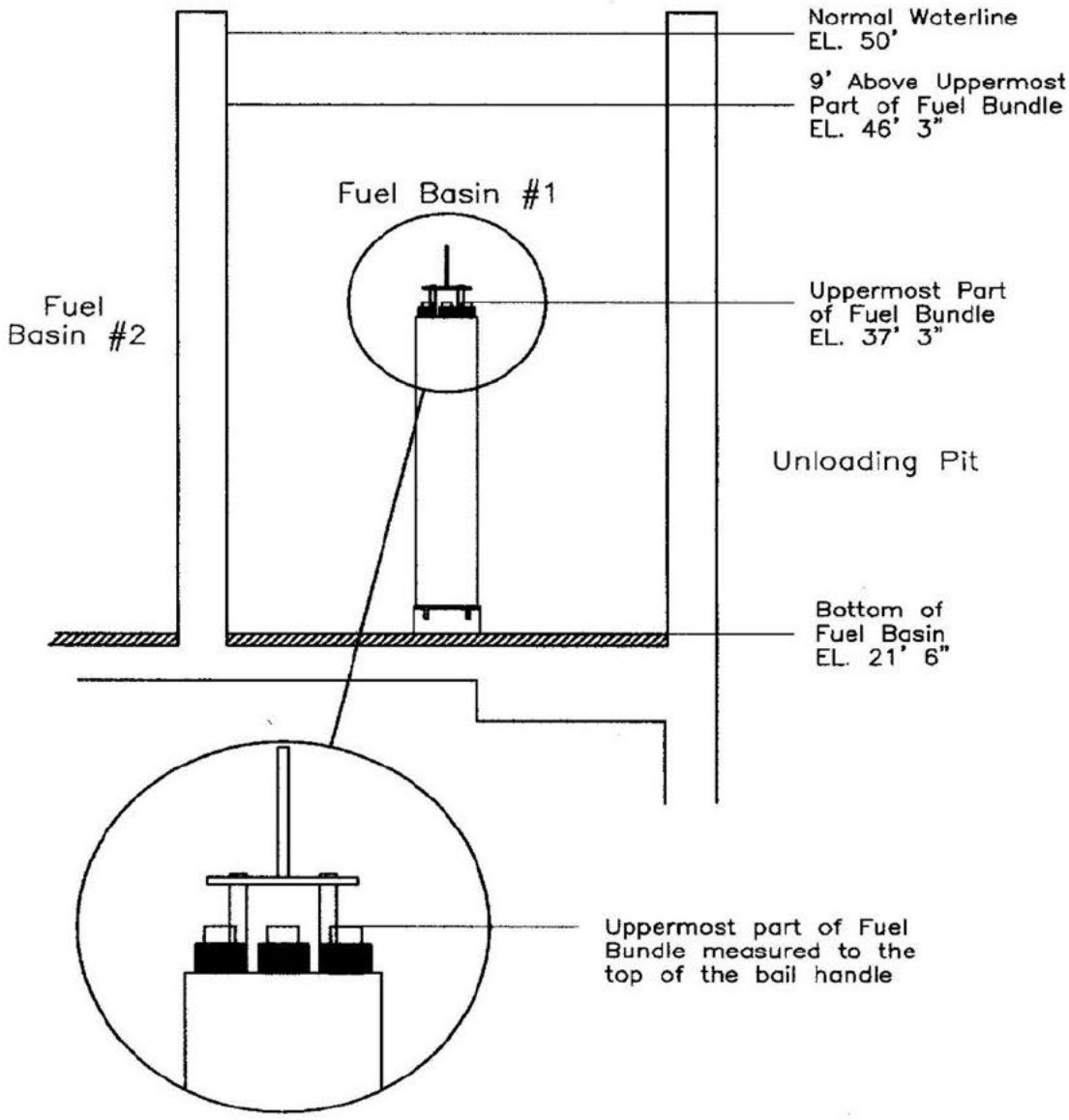

6/2004 FCP

Fuel Basin Map

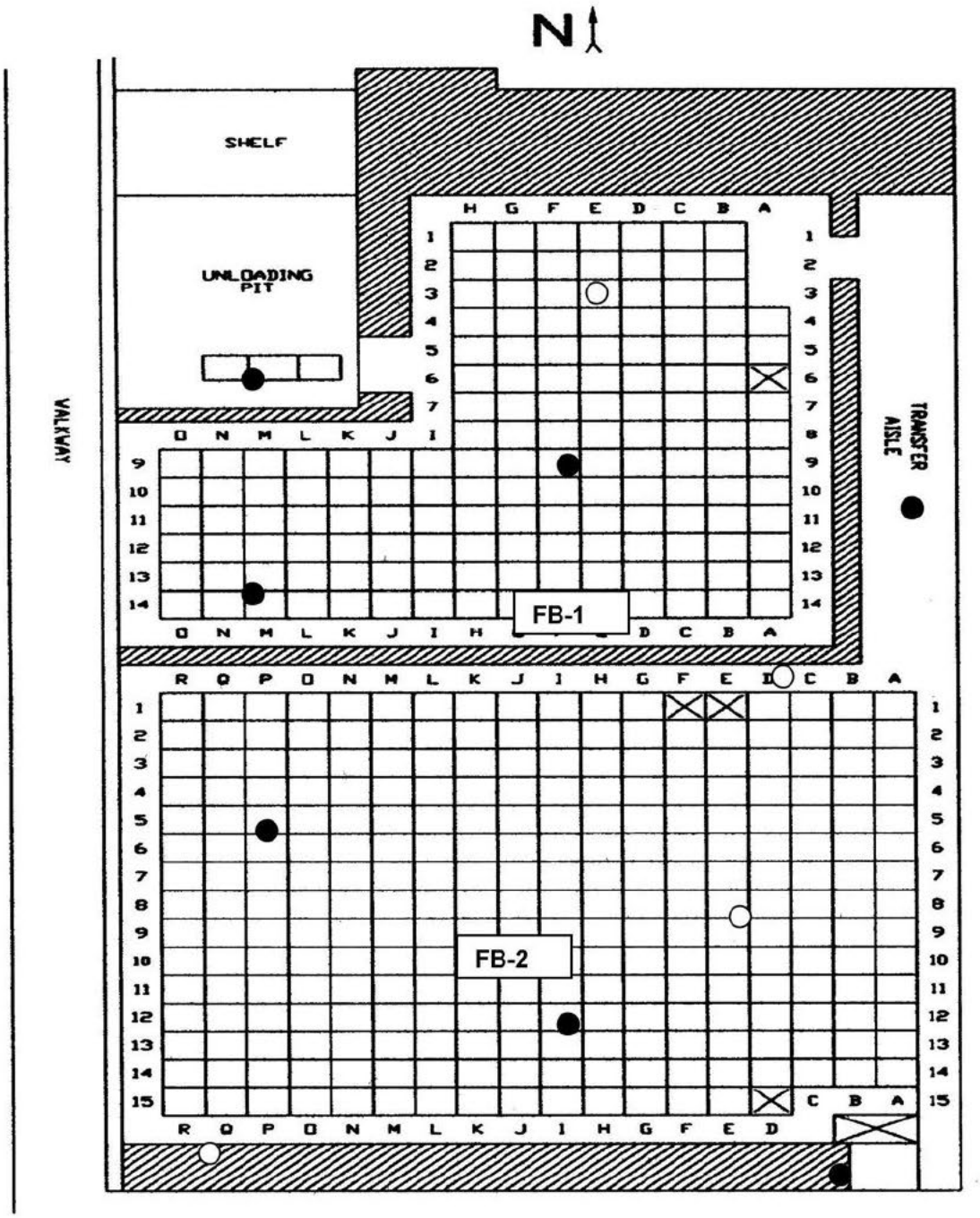

Legend: ● Denotes location where conductivity probe is lowered for data (7 places)

○ Denotes additional locations to take data at conclusion of test.

Basin Start/Finish Conductivity

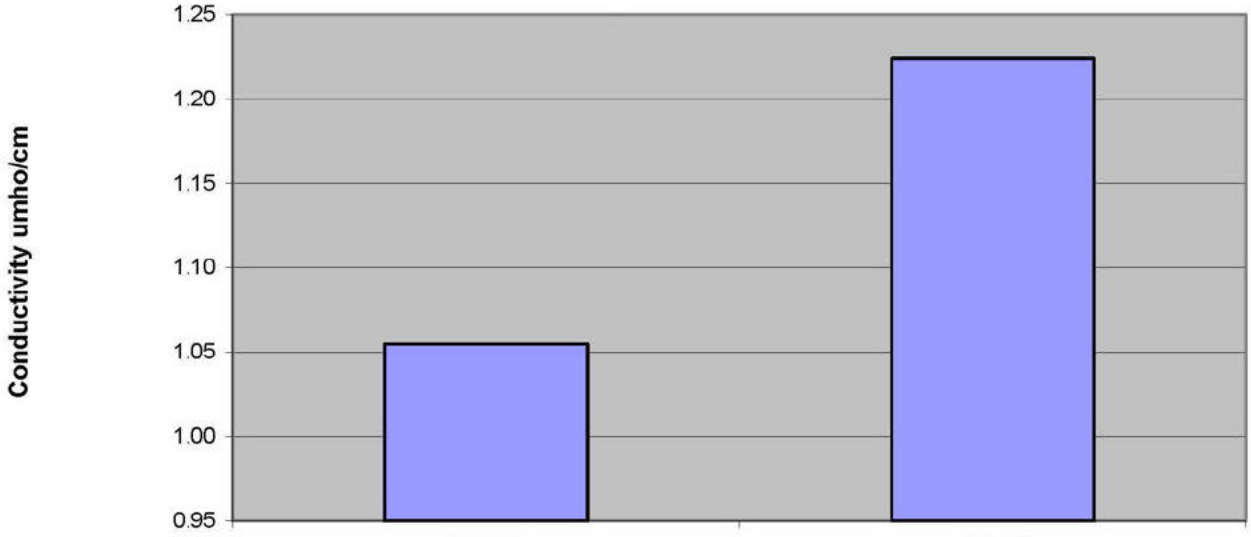

	5/5/04	6/24/04
Conductivity	1.06	1.22

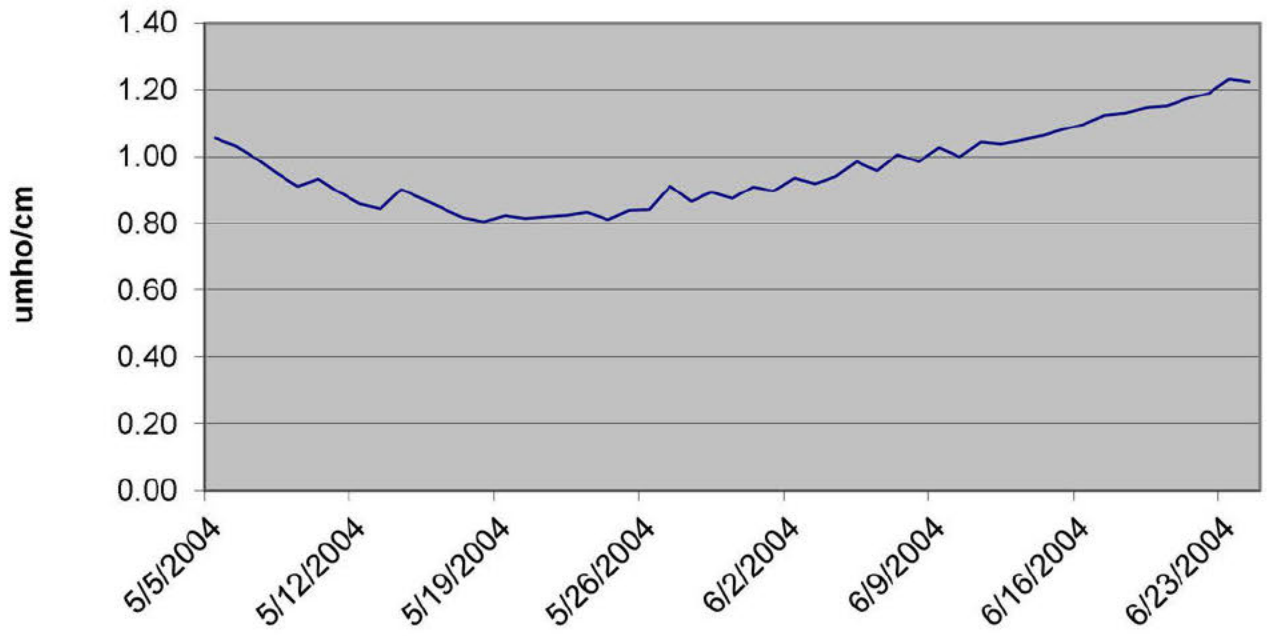
Basin Average Conductivity
umho/cm
1.40
1.20
1.00
0.80
0.60
0.40
0.20
0.00
5/5/2004
5/12/2004
5/19/2004
5/26/2004
6/2/2004
6/9/2004
6/16/2004
6/23/2004

Basin Start/Finish Level

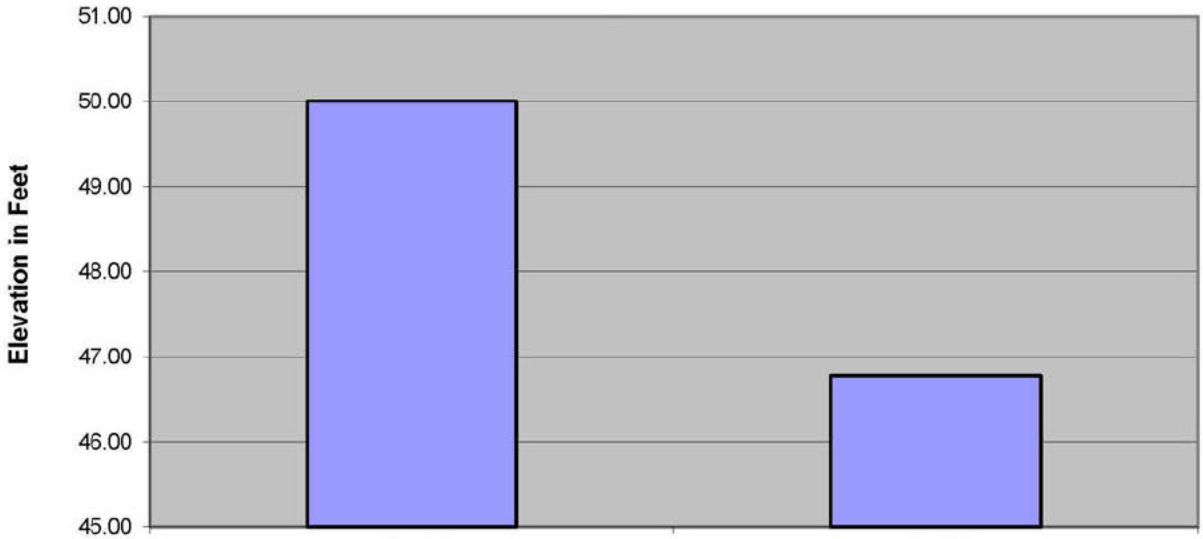

	5/5/04	6/24/04
Level	50.01	46.78

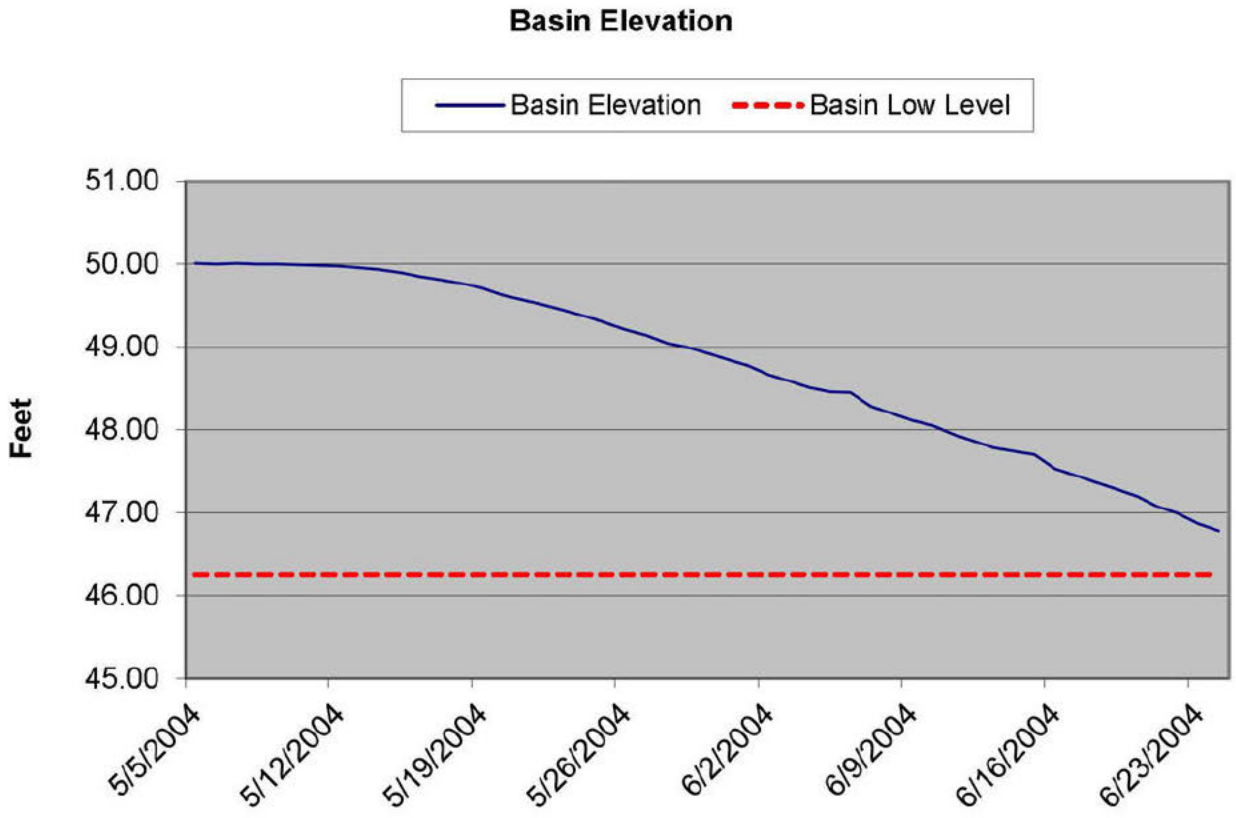
Basin Elevation
Basin Elevation
Basin Low Level
Feet
51.00
50.00
49.00
48.00
47.00
46.00
45.00
5/5/2004
5/12/2004
5/19/2004
5/26/2004
6/2/2004
6/9/2004
6/16/2004
6/23/2004

Basin Start/Finish Temperature

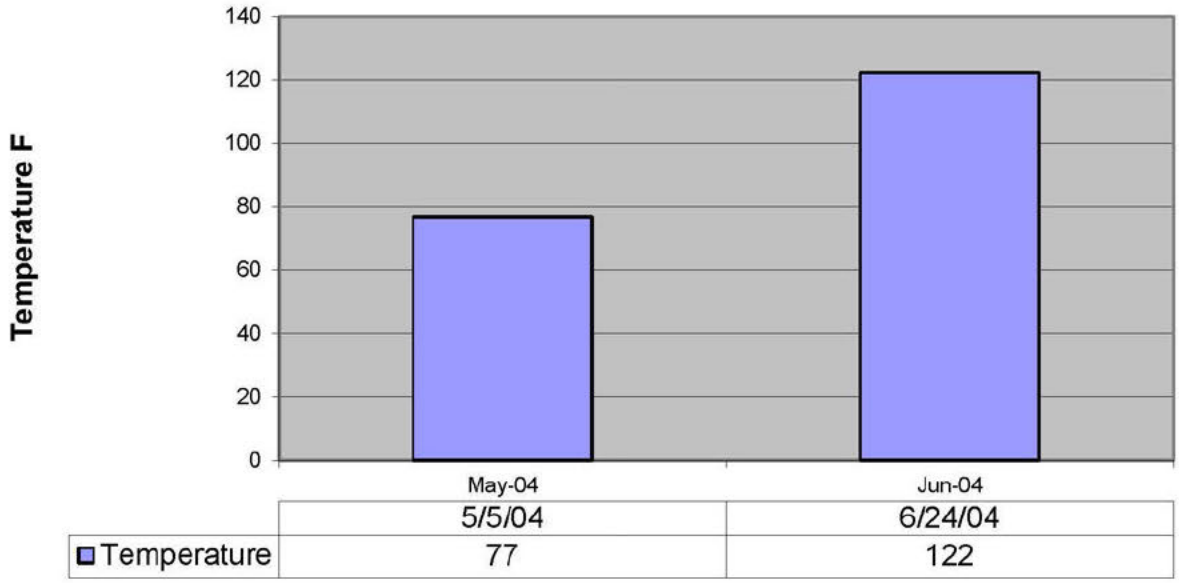

	5/5/04	6/24/04
Temperature	77	122

Basin Average Temperature

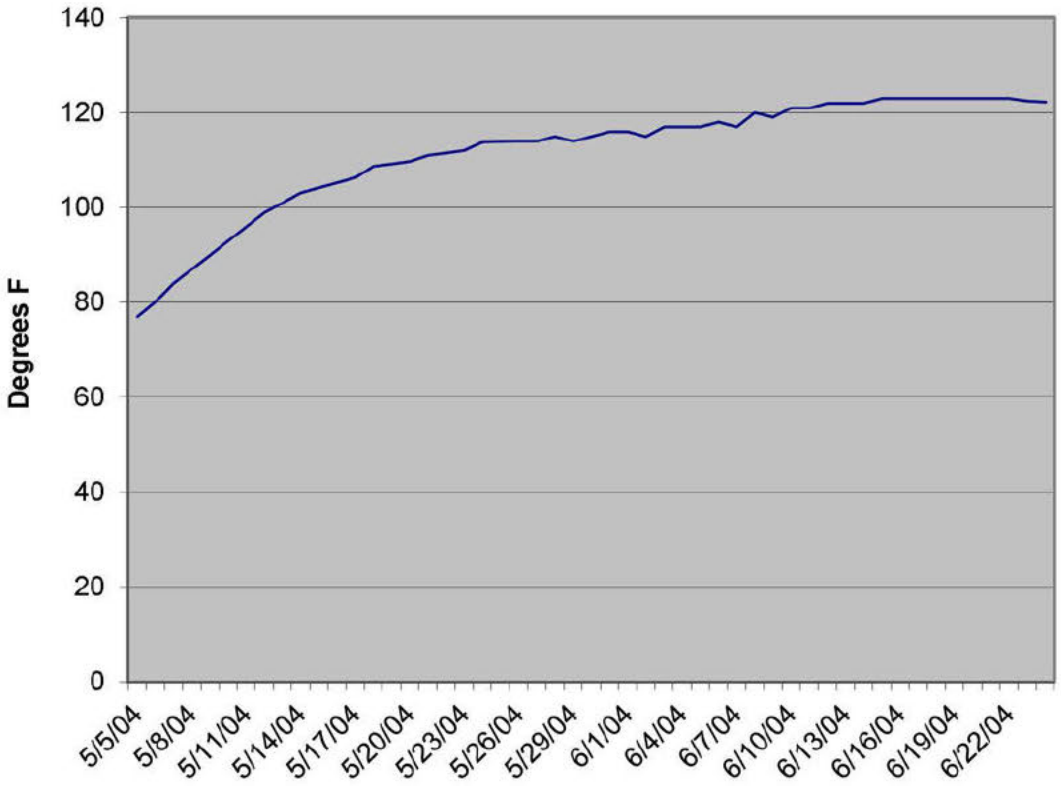

A.10 FUEL BASKET SYSTEM NUCLEAR DESIGN CRITERIA AND BASES

A.10.1 INTRODUCTION

The design criteria for the fuel basket system are as follows:

a. In determination of subcritical limits, the k_{eff} calculated for the most reactive credible conditions shall be less than 0.95 at the 95% confidence level.

b. The initial k_∞ value of fuel to be stored without restrictions other than on the k_∞ value shall not exceed a rod lattice k_∞ of:

   1.37 for 15 x15 PWR fuel bundles (< 8.55 $in.^2$)
   1.41 for 14 x 14 PWR fuel bundles (< 7.80 $in.^2$)
   1.40 for 7 x 7 or 8 x 8 BWR fuel bundles
   1.38 for 10 x 10 BWR fuel bundles (< 5.65 $in.^2$)

c. The k_∞ limit for BWR fuel shall be based on the initial design value of k_∞ (cold, clean fuel) as determined by the fuel designer.

d. The reactivity limit for specification PWR fuel shall be based on the initial cold, clean k_∞, including the poisoning effect of any stainless steel cladding, as determined by the fuel designer or utility customer.

e. For PWR fuel having k_∞ values in excess of the limits for unrestricted storage, the fuel shall have undergone sufficient irradiation to reduce the reactivity to a level below the storage limit taking into account the uncertainties in the calculations of burnup effects.

The k_{eff} for the basin filled with 15 x 15 PWR fuel at k_∞ of 1.37 would be 0.933 as calculated using equations developed by Battelle (Section 5.3.5.3). A k_∞ limit of 1.37 will also allow storage of stainless steel clad fuel enriched to 4.0% U-235 for which k_∞ cold clean would be 1.353.

An additional k_∞ limit has been established for the 14 x 14 PWR fuel since the smaller bundle size results in a lower k_{eff} for a given value of k. A k_∞ limit of 1.41 was established for this fuel since k_{eff} for the basin if filled with fuel at this k_∞ value would be approximately 0.920 at the 95% confidence level.

The rod lattice k_∞ limit of 1.40 for 7 x 7 or 8 x 7 BWR fuel was left unchanged from the original basis for the MFRP to avoid unnecessary changes. The basis for determining k_∞ for BWR fuel (criterion c) considers only cold, clean fuel to avoid the complexity of assessing the reduction in maximum k_∞ value caused by the burnable poison in the fuel. The cold, clean rod lattice k_∞ limit

of 1.40 covers any 7 x 7 or 8 x 8 BWR fuel that might be stored in the fuel storage facilities at Morris Operation (GE-MO).

These design criteria result in limiting the administrative control of fuel receipt largely to fuel identification and evaluation of the cold, clean rod lattice k_∞. The need for determination of the effects of irradiation on the k_∞ value of fuel to be stored should be very infrequent.

The design bases for the fuel basket system are as follows:

a. Criticality evaluations are based on the physical dimensions of specific fuel designs using the largest assembly widths and considering the length to be infinite.

b. The initial U-235 enrichment corresponding to various values of k_∞ was calculated.

c. The poisoning effect of the stainless steel (iron 74%, chromium 18%, nickel 8%, manganese neglected) in the storage basket was included in the criticality evaluation.

d. Fuel centerline location within the storage tube was assumed to be that giving the maximum system reactivity and fuel was assumed to be oriented with the horizontal axes in square array and parallel to the basket axes.

e. The principal criticality calculations were made using a water temperature of 20 °C since the codes employed for the calculations had been most extensively validated at this temperature.

A.10.2 FUEL BASKET SYSTEM - NUCLEAR DESIGN ANALYSIS

The nuclear design analysis was performed by Battelle Pacific Northwest Laboratories[1] using the preceding design criteria and bases and EGGNIT, GAMTEC-11, and KENO-II Monte Carlo computer codes.

Results of the calculations of critical systems to provide validation for the KENO-II code show the code to be slightly conservative (approximately 1.75%). Fuel characteristics are shown in Table A.10-1. The critical systems and calculated results are summarized in Table A.10-2.

TABLE A.10-1
PHYSICAL CHARACTERISTICS OF REPRESENTATIVE LWR FUEL ASSEMBLIES

	1	2	3	4	5	6	7	8	9
Reactor Type	BWR	BWR	BWR	PWR	PWR	PWR	PWR	PWR	PWR
Fuel Designer	GE	GE	GE	B&W	CE	W	W	W	W
Active Fuel Length (in.)	144	144	144	144	137	120	122	144	144
Nominal Envelope (in.)	$(5.438)^2$	$(5.438)^2$	$(5.47)^2$	$(8.536)^2$	$(8.18)^2$	$(7.763)^2$	$(8.426)^2$	$(7.763)^2$	$(8.426)^2$
Rod Array	7x7	7x7	8x8	15x15	14x14	14x14	15x15	14x14	15x15
Rod Pitch (in.)	0.738	0.738	0.640	0.568	0.580	0.556	0.563	0.566	0.563
Rod o.d. (in.)	0.570	0.563	0.493	0.430	0.440	0.422	0.422	0.422	0.422
Clad Material	Zirc-2	Zirc-2	Zirc-2	Zirc-4	Zirc-4	SS	SS	Zirc-4	Zirc-4
Clad Thickness (in.)	0.0355	0.032	0.034	0.0265	0.026	0.0165	0.0165	0.0243	0.0243
Pellet o.d (in.)	0.488	0.487	0.416	0.370	0.3795	0.3835	0.3835	0.3659	0.3659
Radial Gap (in.)	0.0055	0.006	0.0045	0.0035	0.0043	0.0028	0.0028	0.0038	0.0038
H_2O/UO_2 Vol Ratio	1.5476	1.5874	1.691	1.650	1.630	1.4675	1.533	1.717	1.684
Poison Material	Gd_2O_3	Gd_2O_3	Gd_2O_3						

Summarized below are the results of calculations used in establishing the bases for the fuel basket designs.

a. k_{eff} = 0.889 for an infinite system of PWR fuel bundles having the physical dimensions indicated in Column 4 of Table A.10-1, an initial enrichment of 2.6% U-235 (fuel rod lattice k_∞ = approximately 1.33) and in a close-packed square array of full-length, 12 in., Schedule 5, stainless steel pipe canisters at 20 °C water temperature.

b. k_{eff} = 0.774 for an infinite system of BWR fuel assemblies having physical dimensions indicated in Column 2 of Table A.10-1, an initial enrichment of 2.6% U-235 (fuel rod lattice k_∞ = approximately 1.34) and in a close-packed square array of full-length, 8 in., Schedule 5, stainless steel pipe canisters at 20 °C water temperature.

c. For an infinite system of PWR fuel assemblies in four-element fuel baskets, consisting of four 12 in., Schedule 5 pipes in close-packed square array, located on 26.25 in. centers, the effect of fuel assembly location within the pipe canister did not have a significant effect on the system reactivity (ΔK <0.3 of the standard deviation of the calculational method for array reactivity).

d. For infinite systems of PWR fuel baskets as defined in c above, the following relationships among enrichment, fuel lattice k_∞ and system k_{eff} were calculated:

Enrichment (% U-235)	Lattice k_∞	System k_{eff}
1.625	1.2003	0.788 ± 0.006
1.920	1.2504	0.824 ± 0.006
2.295	1.2993	0.864 ± 0.005
2.825	1.3500	0.912 ± 0.006

e. For an infinite system of BWR fuel assemblies in nine-element fuel baskets, consisting of nine 8 in., Schedule 10 pipes in close-packed square array, located on 26.25 in. centers, it was calculated that locating the eight peripheral bundles as close to the central bundle as possible resulted in a maximum increase in k_{eff} of 4.5% over that for fuel at the centerlines for fuel with a lattice k_∞ in the range 1.20 to 1.40.

f. For an infinite system of BWR baskets as defined in e. above, the following relationships between enrichment, fuel lattice k_∞ and system k_{eff} were calculated:

Enrichment (% U-235)	Lattice k_∞	System k_{eff}

1.570	1.2001	0.652 ± 0.005
1.850	1.2500	0.688 ± 0.006
2.210	1.2994	0.732 ± 0.006
3.420	1.3996	0.792 ± 0.007

g. Effects of burnup (fissile material depletion and long-lived fission product buildup) were calculated for BWR and PWR fuels using the LEOPARD code.

A detailed nuclear safety evaluation was made which includes:

- Validation of the correlation between initial U-235 enrichment and rod lattice k_∞ which has been made using the EGGNIT code.

- Correlation of rod lattice k_∞ with bundle array k_∞ (at the reactor bundle lattice pitch). For PWR fuel arrays this difference is very small as the additional water layer at the fuel bundle boundary is approximately 1/16 in. For BWR fuel arrays the effects are somewhat greater as the water layer at the fuel bundle boundary is approximately 0.75 in. Since the safety margins for BWR fuel storage arrays are substantial, the effect does not significantly change the safety of the system.

- Extension of the array calculations to k_∞ of 1.40 for BWR fuel and 1.35 for PWR fuel.

- Evaluation of the effect of elevated fuel and water temperatures.

Additional KENO-II calculations were made to evaluate k_{eff} for PWR arrays at k_∞ (cold) of 1.35 and for temperatures of 20 °C, 50 °C, and 115 °C. It was concluded that temperature does not significantly affect the fuel reactivity.

For BWR fuel containing burnable poison (Gd_2O_3), the value of k_∞ (cold) rises from approximately 1.15 to < 1.25 and declines to < 1.20 by the end of one cycle of irradiation. Thus the presence of poison in the BWR fuel adds to the safety margins in the event of early discharge of the fuel.

Nuclear design analysis for the square tube BWR storage basket was performed by GE^2 to demonstrate the k_{eff} is maintained less than 0.95 with the new square tube geometry. The results of these analyses show that for the worst case abnormal storage condition the maximum k_∞ of 0.836 which is considerably less than the allowed limit of 0.9 k_{eff}.

A.10.3 REFERENCES

1. BPNL, Basin Criticality Safety for MFRP Project-1 Fuel Bundle Storage Baskets, May 1975. (Appendix B.5)

2. GE, Criticality Safety Analysis for Square Tube Fuel Storage Baskets at Morris Operation, May 1987. (Appendix B.15)

A.11 FUEL TO BE STORED -- ADMINISTRATIVE AND TECHNICAL CONTROLS

A.11.1 INTRODUCTION

Administrative control of the k_∞ limits for fuel to be stored at the Morris facility depends primarily on correctly identifying the fuel bundles by number and on assuring that the pre-irradiation k_∞, cold, is less than the limits set by design criterion b[1]. The value for k_∞ is determined principally by the initial U-235 enrichment and to a much smaller degree by the pellet diameter (±0.25%) and the water/fuel volume ratio (±1.3%).

Figures A.11-1 and A.11-2 are used to evaluate the k_∞ value. They were prepared from data provided by Battelle Pacific Northwest Laboratories (BPNL). The form of these charts was designed to avoid the necessity for interpolation and to minimize potential for error in use of the data. When using these charts, the correction factors for variation in water-to-fuel ratio are slightly more conservative (approximately 0.12%) at the higher water-to-fuel ratio than the average value that would be obtained from calculations.

In addition to fuel evaluated as described above, other LWR fuel may be accepted for storage after specific analysis of nuclear characteristics and regulatory approval. For example, fuel from the LaCrosse BWR has been approved for storage after evaluation for storage in the fuel storage system (Figure A.11-1), and for rod lattice k_∞ (Figure A.11-2). Special storage authorizations are included in Chapter 10.

A.11.2 GENERAL PRACTICES

Prior to any transfer of fuel from a reactor site to Morris Operation (GEH-MO), a utility transmits sufficient data on the fuel to be stored to calculate the rod lattice k_∞. The validity of this transmitted data is certified by two qualified individuals from that utility, one being from that organization's quality assurance component. General Electric Company determines the acceptability of that fuel in accordance with Materials License No. SNM-2500 as amended.

A separate confirmation of the fuel identity and initial enrichment is provided by documents required by government regulations. Current NRC policy requires that all transfers of nuclear material be documented on a NRC-741 form, which is initiated by the shipper and completed by the receiver. Copies of the completed NRC-741 form are transmitted to the shipper and appropriate NRC branch within 10 days of receipt, thus verifying the transfer of the material. In order to provide a separate verification of the initial enrichment of each fuel bundle, copies of NRC-741 forms covering shipment of the fuel from the fabricator to the utility will be provided to GE by the utility concurrently with transmittal of the Data for Storage Compliance (Fig. A.11-3).

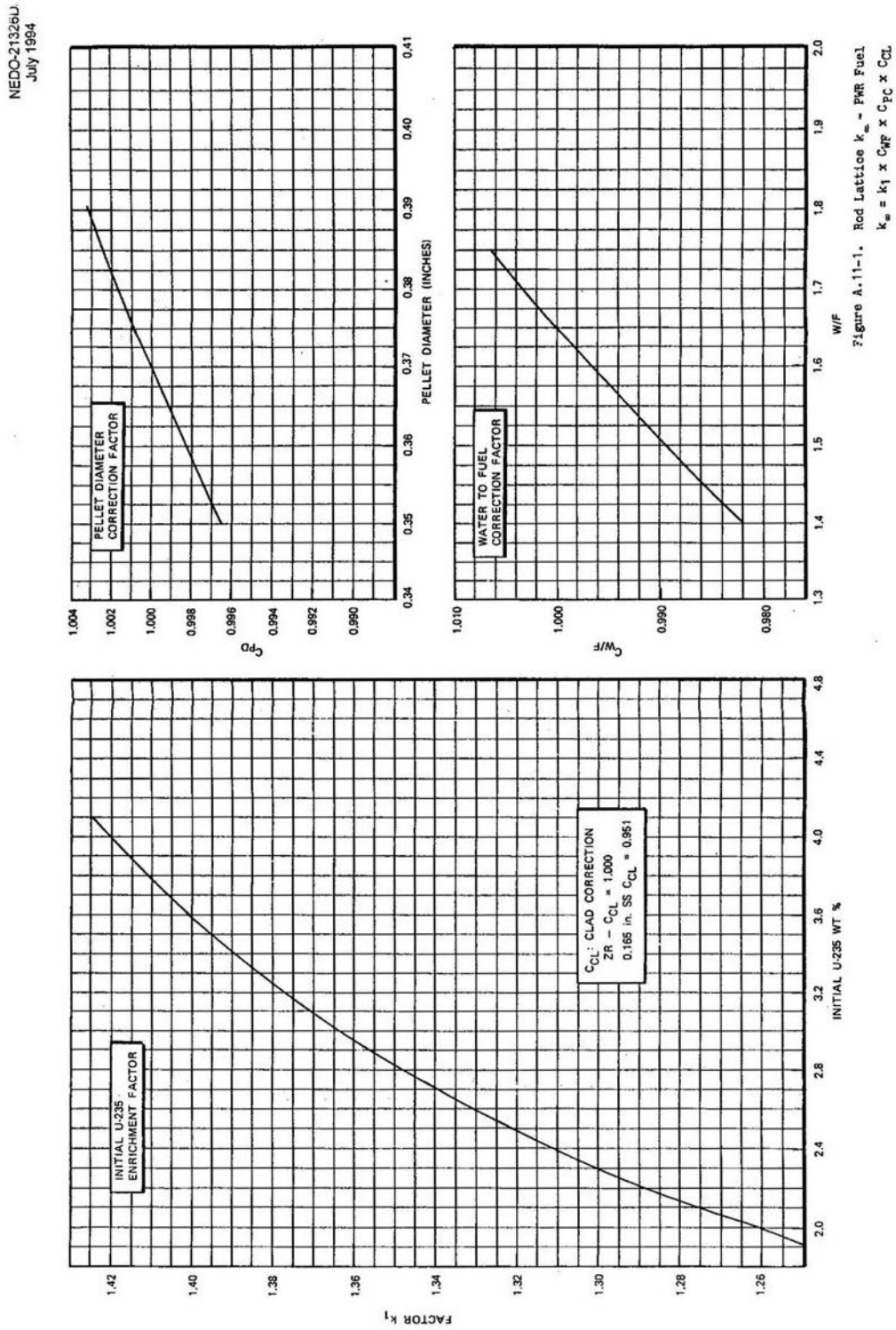

Figure A.11-1. Rod Lattice k_∞ - PWR Fuel
$k_\infty = k_1 \times C_{WF} \times C_{PC} \times C_{CL}$

Figure A.11-2

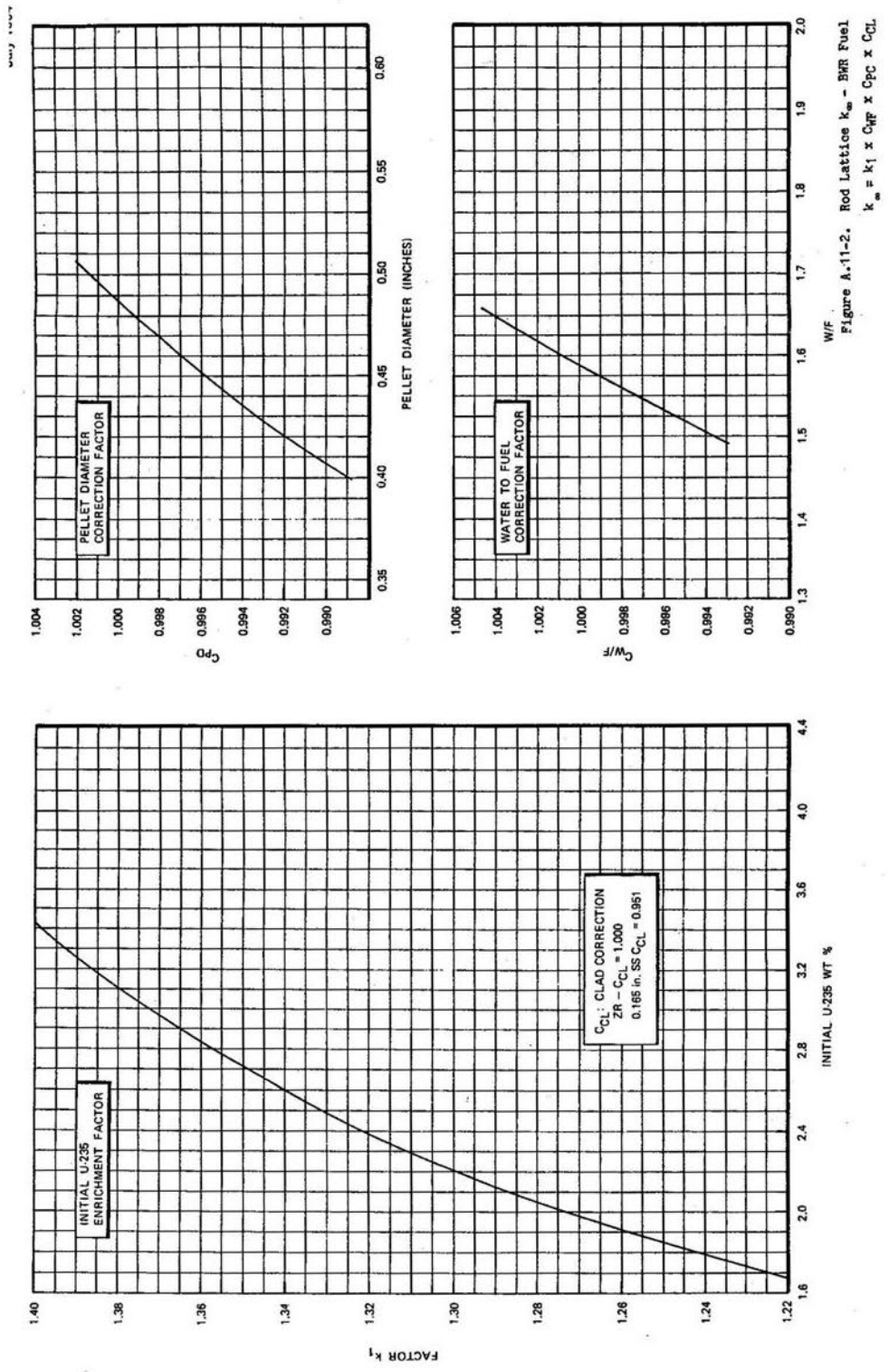

Figure A.11-3. Rod Lattice k_∞ - BWR Fuel
$k_\infty = k_1 \times C_{WF} \times C_{PC} \times C_{CL}$

Figure A.11-3

FIGURE A.11-3
DATA FOR FUEL STORAGE COMPLIANCE
MORRIS OPERATION

==========

Reactor: _____ Bundle Rod Array: _____ x _____

Batch Discharge #: _____ Bundle Dimension: _____ (in.)

Date of Discharge: _____ Cladding Material: _____

Nom. Cladding Thickness: _____ (in.)

==========

Bundle I.D. No.	Total U (kg)	Initial %U-235	Pellet O.D. (in.)	Rod O.D. (in.)	Rod Pitch (in.)	Average Burnup (GWD/MTU)	Final %U-235	Initial Cold, Clean k_{eff} (by Mfg.)	Final k_{eff} Cold, no Xe (if avail)

==========

Data Compiled by:

Signature: _____

Title: _____

Company: _____

Date: _____

Data Verified by QA:

Signature: _____

Title: _____

Company: _____

Date: _____

Prior to shipment, the Plant Manager, or designee, will determine the acceptability of each fuel bundle for storage. This determination will include, but not be limited to, the evaluation of k_∞, using Figures A.11-1 and A.11-2. The rod lattice k_∞ value determined from this evaluation is compared with the bundle k_∞ value received from the contracting utility. The initial cold, clean k_∞ values determined from the evaluation must be less than or equal to the limit set by design criterion b[1] and in agreement with the k_∞ value from the shipper to within 2%. For BWR bundles, the calculated rod lattice k_∞ is compared to the bundle k_∞ from the shipper plus 0.052. For PWR bundles, the calculated rod lattice k_∞ is compared to the bundle k_∞ from the shipper since the rod lattice and bundle k_∞s are essentially the same.

Should General Electric's evaluation determine that the k_∞ of any fuel bundle differs from that value stated by the contracting utility by more than 2%, shipment of that fuel bundle shall be deferred until such time as the difference is resolved and its acceptability established in a manner equivalent to that outlined above. Upon determination that the fuel is acceptable, the General Electric Company will notify the contracting utility that the fuel bundle is acceptable and that it can be shipped.

At the time a fuel bundle is to be shipped to GEH-MO, its identity is checked and verified against the approved list by two individuals of the contracting utility and documented on the shipping release forms. A copy of this list is maintained in the permanent records at GE-MO.

Upon receipt at GEH-MO, the Operations and Maintenance Coordinator (O&MC), or designee, verifies that the bundle listed on the Shipping Report form is one of the approved bundles for receipt. This verification is documented and maintained in permanent files at GEH-MO. The cask is then released to the cask receiving area.

During cask unloading operations, the identity of the fuel is determined and verified by the O&MC or designee. The fuel bundles are then transferred to their assigned locations in the fuel storage basin. The identity and locations of the bundles in the basin are documented in a computer database.

The procedures described above provide sufficient control to ensure fulfillment of the double contingency policy. Each action or transaction is verified by two competent representatives of the organization primarily responsible for that act. The independent review and analysis by General Electric personnel provides further checks on the validity of the data transmitted by the contracting utility and the ultimate acceptability of each fuel bundle. The bundle identity is verified by a minimum of four individuals and documented on at least three forms. As the General Electric Company's evaluation of rod lattice k_∞ is most sensitive to initial enrichment of the fuel bundle, copies of the NRC-741 forms, initiated by the fabricator, will be provided by the contracting utility to assure that the initial enrichment value used as a base for k_∞ is correct.

A.11.3 BWR AND PWR FUEL QUANTITIES

To permit some flexibility in the relative amounts of BWR and PWR fuel to be stored at the Morris facility, the fuel baskets are designed to have a common base and hold-down mechanism. The fuel basket designs accommodate either nine BWR bundles in 8 in. stainless steel pipe or four PWR bundles in 12 in. stainless steel pipe.

Preliminary calculations by BPNL showed that 15 x 15 PWR fuel having k_∞ of 1.35 would give an array k_{eff} of approximately 0.90. A k_∞ limit of 1.35 was used as the basis for the basket detailed design to allow some margin for dimensional tolerances and for any uncertainty in the final design calculations. The completed analysis showed that for k_∞ of 1.35, k_{eff} at the 95% confidence level would be 0.917. At k_∞ of 1.4008, k_{eff} would be 0.952 at the 95% confidence level. Thus the entire basin could therefore be used to store 15 x 15 PWR fuel limited to a k_∞ of 1.37 in an "unrestricted manner."

The k_∞ limits set by design criterion b[1] provide reasonable assurance of meeting near-term utility needs without restrictions other than reactivity. Should a need arise for storage of a limited amount of slightly more reactive fuel, it could be accommodated safely by requiring the fuel have undergone sufficient burnup to assure that k_∞ is below the limit set by design criterion b[1].

A.11.4 CRITICALITY PREVENTION

Protection against accidental criticality in the fuel storage system is provided by:

a. Administrative controls limiting the enrichment and reactivity of the fuel as fabricated.

b. comparison of fuel identity upon receipt to shipping data to ensure that it meets specified limits on enrichment and reactivity.

c. fuel basket design which assures safe spacing between fuel bundles and between fuel baskets even in the unlikely event that fuel basket should be dropped; and

d. moving fuel between the fuel unloading basin and the storage basins only in fuel storage baskets and by handling individual fuel bundles one at a time.

Before a fuel shipment is scheduled for shipment to the GEH-MO facility, the serial number and initial or maximum reactivity (cold k_∞) for each fuel bundle will be stated and certified by the utility. These values will be reviewed and compared to correlations provided by BPNL. (See Section 5.3.5.6.)

PWR fuel having a cold, clean k_∞ in excess of the limits established by design criterion b[1] is classified as non-specification fuel in the standard fuel storage contract, which is the basis for

establishing the conditions for fuel storage at the Morris Operation. Presently, there is no PWR fuel contemplated for storage which would have a k_∞ in excess of the specified limits. For such non-specification fuel to be included under the contractual arrangement for storage, it will be necessary to establish that the post-irradiation value for k_∞ is confirmed to be less than the limiting value set by design criterion b. The evaluation of pre-irradiation k_∞ will be made based on the BPNL correlation of enrichment versus k_∞ adjusted as appropriate for pellet diameter and water-to-fuel ratio. The amount of irradiation required to assure that the post-irradiation k_∞ is less than the limit set by design criterion b[1] will be ascertained using the pre-irradiation k_∞ and BPNL correlations.

A.11.5 REFERENCES

1. Refer to A.10.1, a through e.

A.12 FUEL BASKET SYSTEM DESIGN ANALYSES

The fuel unloading and storage basins at Morris Operation (GEH-MO) are designed in accordance with earthquake and tornado criteria as described in Chapter 4. General criteria also apply to the design of the fuel basket system:

a. No deformation or damage shall occur to the concrete or to the liner that would result in significant leakage.

b. There shall be no piping or penetration failure that would lower water level significantly.

c. Cranes may be derailed, but must not fall into the basins.

d. The enclosure framework above the basin must remain essentially intact.

e. Handling and storage areas shall withstand contact or impact with stored materials.

The fuel basket system design is consistent with the response spectra specified in Regulatory Guide 1.60 and dampening values specified in Regulatory Guide 1.61.

Because the supporting grid system transmits earthquake forces to the basin walls, the basin structure has been analyzed to ensure that these forces are adequately carried.

Design analyses have been performed under General Electric direction as follows:

a[1]. Manual static analyses of
  (1) Grid support structure
  (2) Latch Mechanism
  (3) Fuel basket

b[1]. Computer analysis of the grid:
  (1) Natural frequency analysis
  (2) Dynamic model analysis
  (3) Static load analysis

c[1]. Thermal analysis of the grid
d[1]. Analysis of friction loading on the latch mechanism
e[1]. Static load test of the latch mechanism
f[2]. Dynamic load test of the latch mechanism
g[3]. Effects from pilot model spacing and section changes
h[3]. Load effects on basin walls and liner from pilot model changes
i[3]. Unloading pit basket retainer frame
j[3]. Basket lifting tools (yokes)

A.12.1 REFERENCES

1. Programmed & Remote Systems Corporation (PaR), Fuel Storage System Design Report - GE Morris Operation, April 1975. (See Appendix B.16)

2. Construction Engineering Research Lab, Seismic Shock Environment Test of Simulated Nuclear Fuel Storage Basket, Department of Army, August 1975 (Technical report M-150). See Appendix B.

3. Supplement 1, Fuel Storage System Design Report - GE Morris Operation, General Electric, May 1975 (no publication number). See Appendix B.

A.13 CASK DROP ANALYSES

A.13.1 INTRODUCTION

Two analyses were made to assess the effects of a cask drop: a cask drop on the cask unloading pit shelf, and a cask drop to the floor of the unloading pit.

In considering the integrity of basin structures, it should be noted that the cask unloading pit area of the main process building rests directly on an underlying shale bed. Tests of this rock structure indicate ultimate compressive strengths of 6,000 to 11,000 lb./sq. in. Therefore, the limiting material in regard to ability to absorb cask drop forces is the 3 ft. 10 in. thick foundation, which is constructed of 3,000 psi design concrete having 28-day break test values in excess of 4,500 psi. The floor of the unloading pit is lined with 1/4 in. thick stainless steel sheet supported on a steel plate 1 3/4 in. thick to resist puncture and to distribute cask forces over the concrete surface. The unloading pit shelf (refer to Section 5.3.4) is lined with 1/4 in. thick stainless steel sheet, directly on the concrete, over which is located a 2 in. thick load distribution plate and an energy-absorbing pad.

A.13.2 CASK DROP ON THE SHELF

Analyses of the potential dropping of a shipping container onto either the floor of the unloading pit or the floor of the unloading pit shelf considered the effect of such an accident on both the container and the basin structure. For the purpose of the analysis it was assumed that the accident would involve the IF-300 shipping cask, which was the largest shipping container for irradiated LWR fuel then in use. Further, it was assumed that the cask would strike in such a manner as to allow minimum energy absorption by the shipping container fins and therefore the highest loading on the floor.

NOTE: It should be noted that when the use of casks to ship fuel is again considered, these analyses for cask drop should be reviewed, based on the cask proposed for shipment.

A.13.2.1 Impact Pad

The floor of the shelf in the cask unloading pit is protected by a pad that consists of a 1 in. thick stainless steel plate welded to 4 in. high x 1/2 in. thick stainless steel fins designed to crush at a predicted force, thereby limiting the force imposed on the floor to acceptable values. The pad is designed to crush at a force of 1.2×10^7 lb., where a force of 1.8×10^7 lb. is required to deform the fins on the IF-300 cask. Thus, the total energy of the drop must be absorbed by the pad. The pad is placed on a 2 in. thick floor plate consisting of two 1 in. thick stainless steel plates.

A.13.2.2 Drop Height and Energy

The maximum lift height and therefore drop height assumed is 1 ft. above the wall between the decontamination area and the unloading pit. The impact height (h_w) will be equivalent to 21.5 ft. of water (2 ft. in air, equivalent to 3 ft. in water, plus 18.5 ft. in water). The final velocity of impact (v_2) is found by conservation of energy:

$$(F_n)(h_w) = \left(\frac{1}{2}\right)(m)(v_2)^2 \qquad \text{(A.13-1)}$$

where:

F_n = net force, and

m = mass.

The net force, F_n, can be calculated by summing the forces of gravity, buoyancy and drag in the vertical direction. The buoyant force, F_B, is calculated from the equation.

$F_B = \rho V$

where

ρ = density of water

V = volume of cask.

The drag force (F_D) is calculated from an equation given in Mark's **Handbook of Mechanical Engineering**, Section 11, page 72.

$$F_D = (C_D)\left(\frac{1}{2}\right)(\rho)\left(\bar{v}\right)^2(A)$$

where

C_D = drag coefficient;

ρ = density of water;

$\bar{v}$ = average velocity and

A = cross-sectional area of cask.

The value of C_D is 1.1, which is found in Vennard's **Fluid Mechanics,** pages 516-517. The average velocity ($\bar{v}$) is calculated as follows:

$\bar{v}$ = 1/2 ($v_0 + v_2$). Since $v_0 = 0 = \bar{v} = 1/2\ (v_2)$.

v_2 = impact velocity

Substituting the dimensions and weight of the IF-300 container into Equation A.13-1 gives v_2 = 33.6 ft./sec. The equivalent height in air, h_e, is:

$h_e = (v_2)^2/2g = 17.5$ ft.

The total impact energy (E) is described by the equation:

$E = Wh_e$

where:

W = weight of the cask = 146,000 lb. (includes the yoke).

The total impact energy of the cask is found to be 2,555,000 ft-lb. (3.07×10^7 in.-lb.).

A.13.2.3 Fin Bending Data Analysis

In 1970-71, ORNL conducted a series of tests to determine the energy absorbing capability of steel fins under impact, large deformation conditions. The results of his work are reported in ORNL TM-1312 Vol. 9. This work is the source of fin deflection and impact force calculations used in the General Electric analysis.

General Electric applied details of the 0° tests for use in designing the energy absorbing fins for the IF-300 cask. A correlation was developed from the tests which permitted GE to estimate cask stopping distance (hence deceleration) given cask kinetic energy, fin material and fin geometry. This same correlation was also used to estimate the deflection of the impact pad fins used to protect the shelf in the GEH-MO unloading basin. A summary of this correlation and the method used for the analysis follows:

In tests, specimens were mounted on an instrumented load cell and impacted by guided falling weights dropped from various heights. Test data was recorded on an oscilloscope and photographed, from which force-time relationship graphs were plotted.

Test specimens mounted vertically always formed two hinges. (See Figure A.13-1.) Specimens inclined 10° with the vertical formed two hinges with about 85% frequency; the remainder only one hinge. At angles somewhat greater than 10°, one hinge was always the case. Test specimens tabulated in Table A.13-1 were all mounted vertically and formed two hinges.

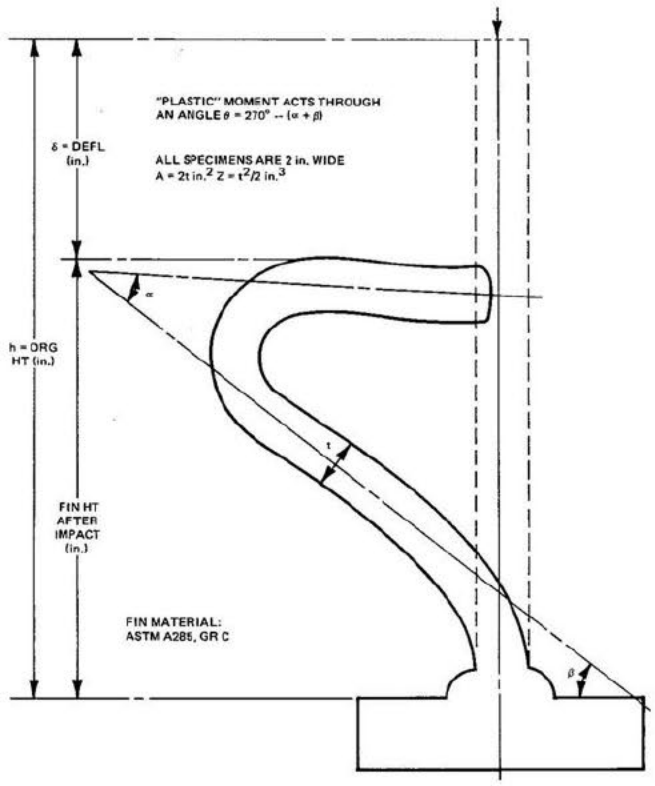

Figure A.13-1. Traced Profile of Specimen No. 5 After Impact (Typical)

In evaluating the test results, reference was made to **NACA Technical Note No. 868,** Figures 25 and 35 (copies of which are included as Figures A.13-2 and A.13-3, respectively) to determine the "hinge" stress level.

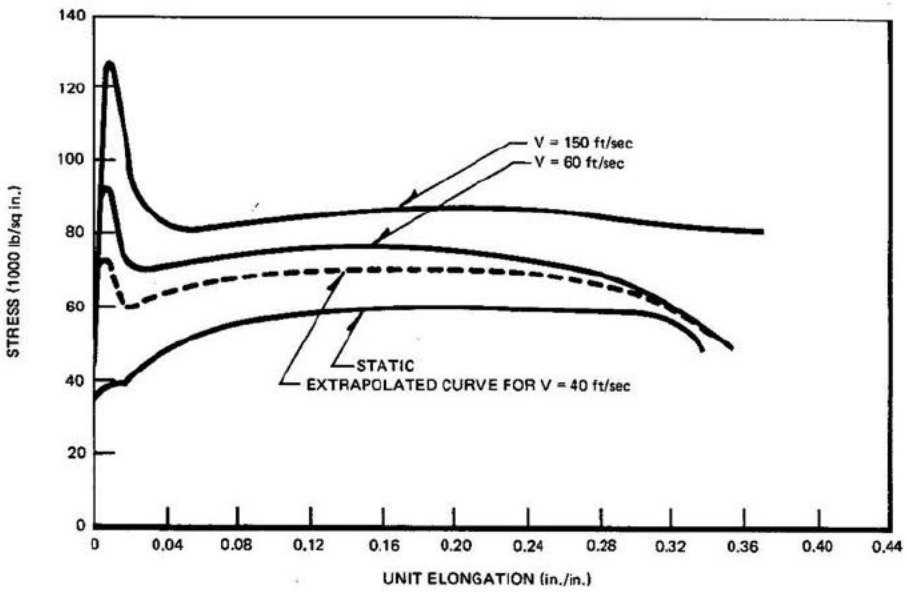

Figure A.13-2. Stress Strain Curves, Hot Rolled Steel

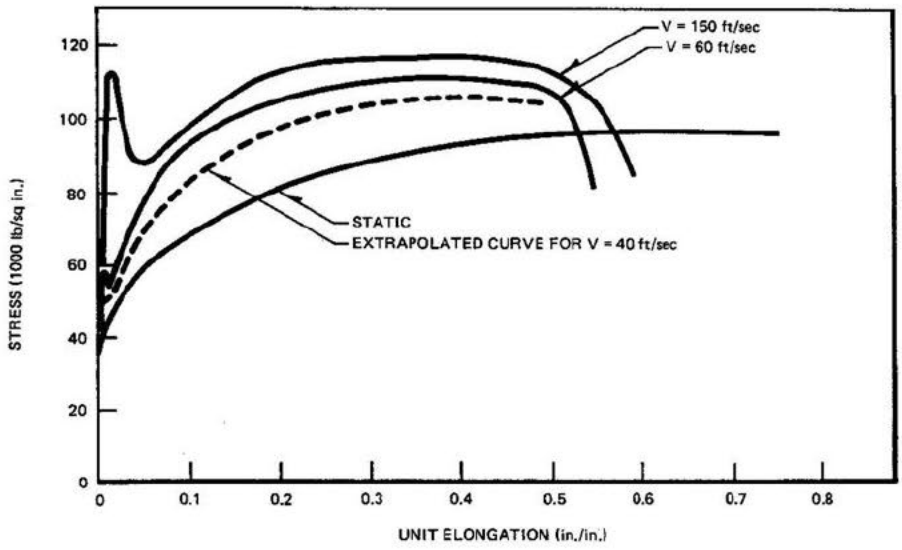

Figure A.13-3. Stress Strain Curves, 18-8 Stainless Steel

Referring to Figure A.13-2 for hot-rolled steel, the properties of which closely resemble those of ASTM A285, Gr C, of which the test fins were made, a hinge stress of σ_H = 65.0 ksi[a] was chosen as representing a reasonable value for the velocities involved, Likewise, for ASTM A240, Type 304L (18-8 stainless steel), σ_H = 90.0 ksi (Figure A.13-3).

a Thousand pounds = kip, Thousand pounds per square inch = ksi

Energy of Bending:

$$E_m = M\theta \qquad M = \sigma_h z \qquad Z = \frac{bt^2}{4}$$

where:

M is the plastic moment

θ is defined in Figure A.13-1

b is fin width (inches)

t is fin thickness (inches)

and $$E_m = \frac{\sigma_H bt^2\theta}{4} inch - kip$$

For A285, Gr C: $$\theta = \frac{E_m}{16.25bt^2}$$ (test fins)

For A240, type 304L: $$\theta = \frac{E_m}{22.5bt^2}$$ (cask fins and pad fins)

Referring to Table A.13-1 and the columns headed E, E_m and E_p (E_p = E - E_m), it is noted that E_p (absorbed energy not accounted for by calculated bending) represents, with only one exception, more than 50% of the total external drop energy, "E". In evaluating the fins, it was conservatively assumed that "E_p" accounts for only one-half of the total energy.

In order to determine the fin height after impact, it was necessary to establish the empirical relationship between θ, δ, and h. (See Figure A.13-1.) This was done by calculating the percentage of δ to h and plotting against θ. As noted in Figure A.13-4, reasonable correlation was developed.

Table A.13-1 TEST SPECIMENS DATA

No.	Fin Size[a] h x t(in.)	δ in.	θ Deg	Rad	Drop Wt (kip)	Drop Ht (in.)	Energy[b] E(in.-k)	Energy of Bndg[b] E_m(in.-k)	$(E-E_m)$[b] E_p(in.-k)	$\frac{100E_p}{E}$	$\frac{100\delta}{h}$	$\frac{l}{r}$	Impact Vel FPS
1	6 x 0.75	2.63			0.472	354.3							
2	6 x 0.75	2.00	177	3.09	0.472	345.3	167.3	56.5	110.8	66.2	33.3	27.7	43.6
3	6 x 0.75	2.56	184	3.22	0.472	354.3	167.3	58.9	108.4	64.8	42.7	27.7	43.6
4	6 x 0.75	1.75			0.472	354.3							
5	9 x 0.75	6.00	268	4.68	0.472	351.3	165.8	85.5	80.3	48.4	66.7	41.5	43.4
6	9 x 0.75	1.75	126	2.20	0.304	351.3	106.7	40.2	66.5	61.4	109.5	41.5	43.4
7	8 x 0.50	3.44	197	3.44	0.178	352.0	62.7	28.0	34.7	55.3	43.0	55.4	43.5
8	8 x 0.50	2.25	151	2.64	0.157	352.0	55.3	21.4	33.9	61.3	28.1	55.4	43.5
9	6 x 0.50	1.25	134	2.34	0.157	345.0	55.6	19.0	36.6	65.8	20.8	41.5	43.6
10	6 x 0.50	1.00	124	2.16	0.157	354.0	55.6	17.5	38.1	68.5	16.7	41.5	43.6
11	6 x 0.50	0.81	101	1.76	0.157	354.0	55.6	14.3	41.3	74.3	13.5	41.5	43.6
12	6 x 0.50	0.69	88	1.54	0.157	354.0	55.6	12.5	43.1	77.5	11.5	41.5	43.6
13	6 x 0.50	0.94	117	2.04	0.157	354.0	55.6	16.6	39.0	70.1	15.7	41.5	43.6
14	3.5 x 0.50	0.13	64	1.12	0.157	356.0	55.9	9.1	46.8	83.7	3.7	24.2	43.7
15	3.5 x 0.50	0.25	107	1.87	0.199	356.0	70.8	15.2	55.6	78.5	7.1	24.2	43.7
16	3.5 x 0.50	0.69	156	2.72	0.241	356.0	85.8	22.1	63.7	74.3	19.7	24.2	43.7
17	3.5 x 0.50	0.75	162	2.84	0.241	356.0	85.8	23.1	62.7	73.2	21.4	24.2	43.7
18	3.5 x 0.50	0.63	147	2.57	0.241	356.0	85.8	20.9	64.9	75.6	18.0	24.4	43.7
20	6 x 0.25	3.12	230	4.02	0.094	180.0	16.92	8.16	8.76	51.8	52.0	83.0	31.1
22	6 x 0.25	3.00	148	2.59	0.094	144.0	13.53	5.26	8.27	61.1	50.0	83.0	27.8
23	4 x 0.25	0.81	131	2.29	0.094	120.0	11.28	4.65	6.63	58.8	20.3	55.4	25.4
24	4 x 0.25	0.69	123	2.15	0.094	144.0	13.53	4.37	9.16	67.7	17.3	55.4	27.8
25	4 x 0.25	1.94	174	3.04	0.094	180.0	16.92	6.17	10.75	63.5	48.5	55.4	31.1
26	4 x 0.25	1.56	187	3.27	0.094	168.0	15.80	6.64	9.16	58.0	39.0	55.4	30.0
27	4 x 0.25	1.44	170	2.97	0.094	168.0	15.80	6.03	9.77	61.9	36.0	55.4	30.0
28	2.5 x 0.25	0.75	170	2.97	0.094	180.0	16.92	6.03	10.89	64.3	30.0	34.6	31.1
30	2.5 x 0.25	1.12	203	3.54	0.094	216.0	20.30	7.19	13.11	64.5	44.8	34.6	34.1
31	2.5 x 0.25	0.87	190	3.32	0.094	216.0	20.30	6.74	13.56	65.8	34.8	34.6	34.1

[a] All test fins are 2 in. wide.
[b] in.-k = thousand inch-pounds

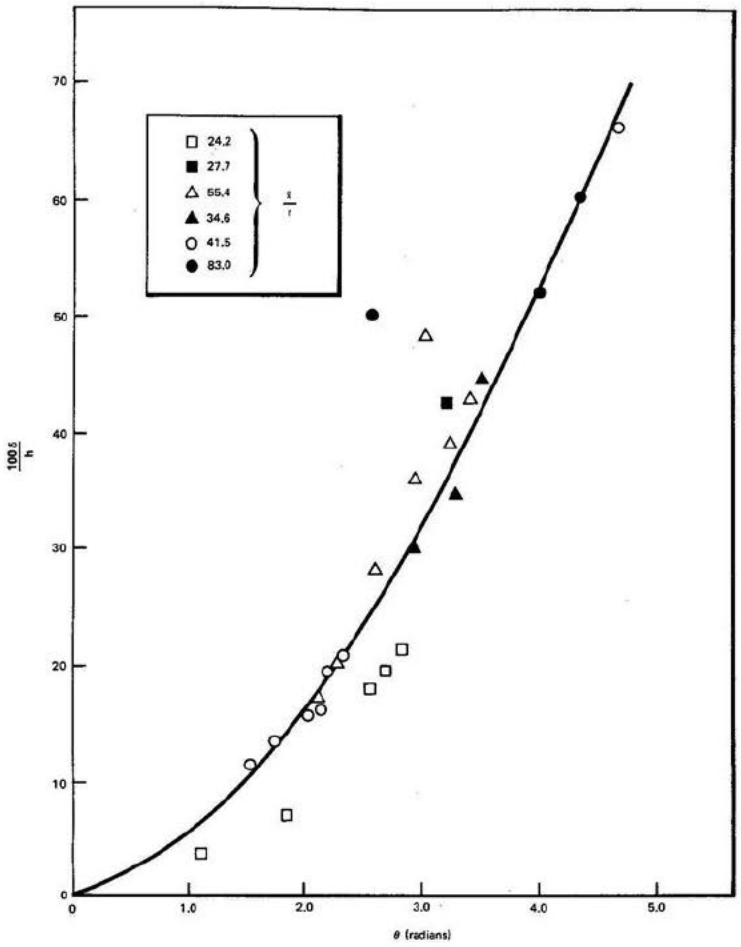

Figure A.13-4. Empirical Relationship Between θ, δ and h

Use of the Correlation

Using Figure A.13-1 as an example:

$$\theta = \frac{E_m}{16.25bt^2}$$

E = 165.8 inch-kip

E_m = 1/2 (165.8) = 89.2 inch-kip

b = 2 in. fin width

t = 0.75 in. fin thickness

$$\theta = \frac{(82.9)\ inch - kip}{(16.25)(2)(0.75)(2)} = \quad = \quad 4.53 \text{ radians}$$

From Figure A.13-4 at θ = 4.53

$$\frac{100\delta}{h} = 62.5$$

Since h = 9 in. $\quad \delta = \frac{62.5}{100}(9) = 5.63$ in.

This correlates very well with the measured deflection of 6 in. for fin No. 5.

The g loading for this fin would be defined as:

$$g = \frac{\text{Drop Height}}{\text{Stopping Distance}}$$

$$= \frac{351.3 \text{ in.}}{5.63 \text{ in.}}$$

$$= \quad 62.4$$

This is compared to 59 g based on actual deflection and therefore the correlation is somewhat conservative. It is very conservative based on measured average forces, Figure A.13-5.

The method described above was applied to the design of the GEH-MO unloading pit shelf impact-absorbing pad.

A.13.2.4 Impact on Step Corner

The impact-absorbing pad on the floor of the step of the unloading pool has been designed to limit the forces of a falling cask and distribute these forces over a large area. The pad on the step extends to the front edge and to a point 6 in. from each wall. The space between the pad and wall is not large enough to allow the cask to hit an unprotected part of the floor.

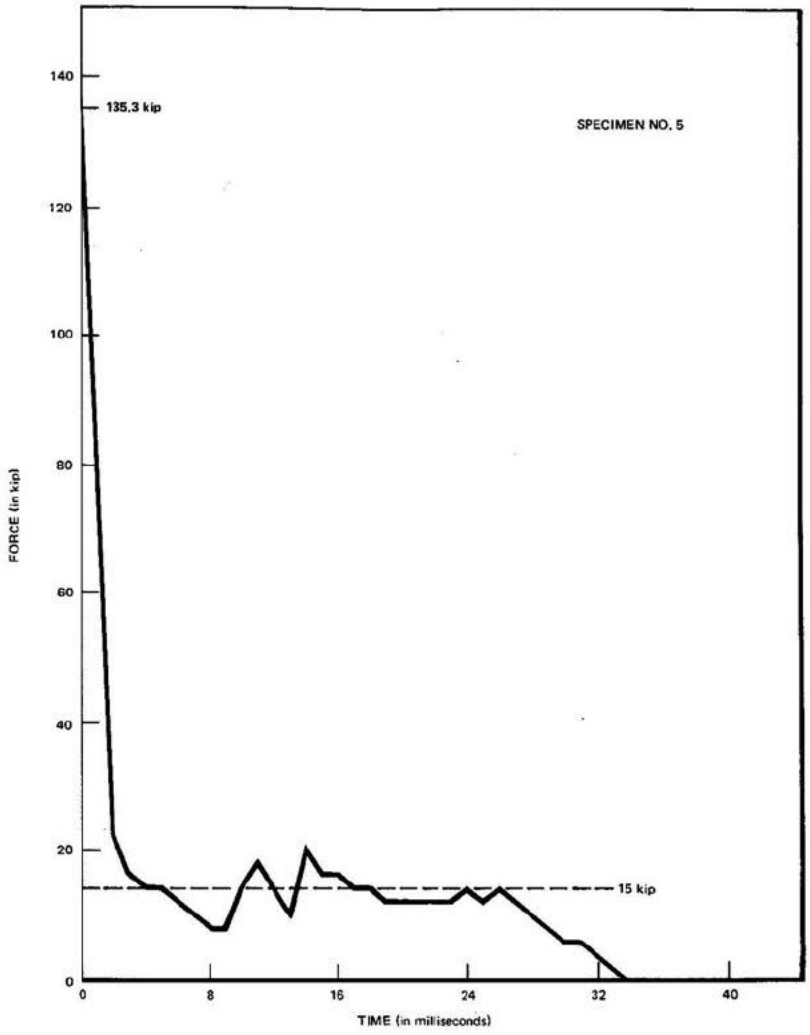

Figure A.13-5. Force-Time Curve for Specimen No. 5

The maximum load that the corner of the step could experience from a falling cask is when the cask's center of gravity is located directly above the edge at the time of impact. Stresses in the concrete foundation that result from such an accident are analyzed by calculating the forces developed as the energy is absorbed by the impact-absorbing pad. As the kinetic energy is absorbed, the load on the concrete from the resultant force is distributed by the impact pad, and the 2 in. floor-plate, over an area that is considerably larger than half the cross-sectional area of the cask.

The impact-absorbing pad is constructed of a top plate, 1 in. thick, welded to fins that are 1/2 in. thick and 4 in. long (see fin orientations in Figure A.13-6). The pad is placed on a 2 in. thick

floor plate consisting of two sheets, each of which is 1 in. thick. All the construction material is 304L stainless steel.

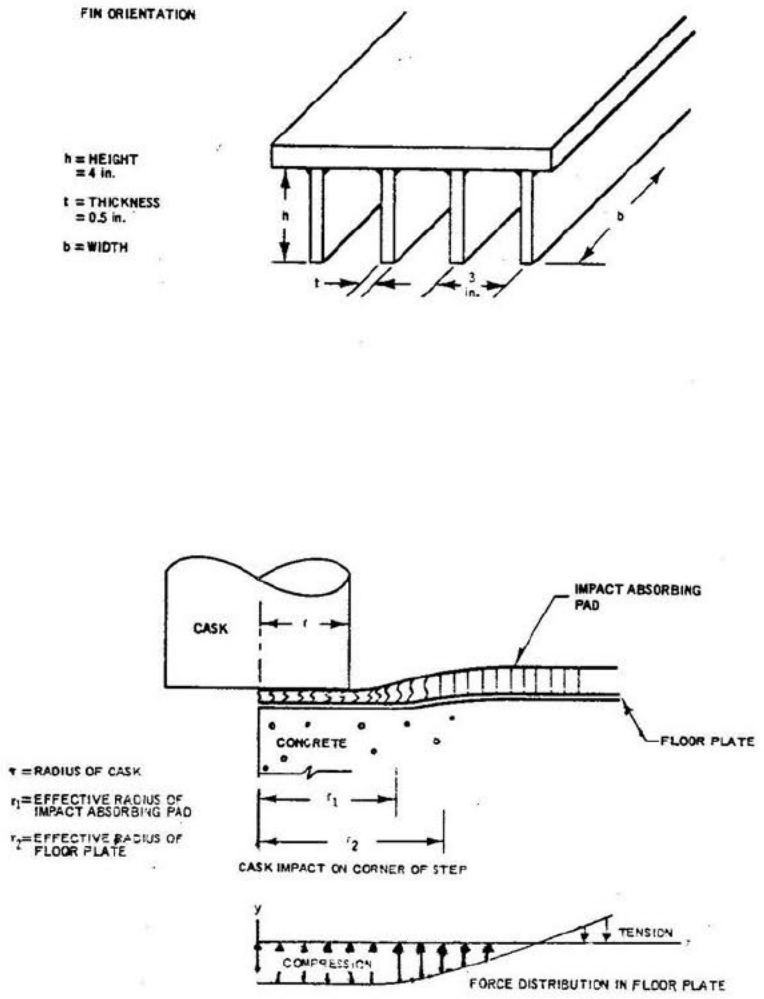

Figure A.13-6. Fin Orientation

When the cask hits the pad there is a radius on the flat plate beyond the cask where the compressive forces change to tension[1] (Figure A.13-6). At that point the force is zero. By taking a weighted average of fin deflection as a function of force, the effective radius is found to be 4.75 inches more than the cask radius or 39.86 inches. From this effective radius, the total width of affected fins is calculated to be 697.6 in.

The angle θ through which the plastic moment acts when a fin bends is given by the equations:

$$\theta = \frac{E_m}{22.5t^2} = 3.90 \text{ radians}$$

where

E_m = half the total drop energy (1.53×10^4 inch-kips)

t = fin thickness (0.5 inch)

The deflection (δ) is calculated by using the correlation given in Figure A.13-4. For $\theta = 3.90$, $100(\delta)/h = 50.5$ and h = 4 inches:

$\delta = 4(50.5)/100 = 2.02$ in.

The g-loading then for a 17.5 ft drop is:

$$g = \frac{H_e}{\delta_i} = \frac{17.5 \times 12}{2.02} = 104g$$

This means that a force of 104 g is imparted to the IF-300 container as a result of the 17.5 ft. drop. Since a force of 272 g is required to bend the IF-300 fins in an end drop on an unyielding surface, the fins on the IF-300 will not deform as a result of the drop onto the impact pad.

Results of tests conducted by Atchely and Furr[2] indicate that the ultimate dynamic load for concrete is 1.5 times greater than the ultimate static load. The ultimate static load indicated by the 28-day test[3] is 4,634 psi. Therefore, the ultimate dynamic load is 6,951 psi. Under this load, maximum deflection of reinforced concrete is approximately 2.317×10^{-3} inches. From "flat-plate" theory, the maximum effective radius that results from the 2 in. floor plate is 2.96 inches more than the effective radius of top plate of the pad (39.86 inches). By taking a weighted average of the deflection as a function of force, the average effective radius is 42.795 inches. The effective area, A_e, on the concrete is:

$A_e = (\pi/2)(42.795)^2 = 2{,}876.7$ in.^{2}

The load experienced by the concrete that results from the impact force (F_I) is:

$L = F_I/A_e$

$$F_I = \frac{E}{\delta} = \frac{3.07 \times 10^7 \text{ in.-lb.}}{2.02 \text{ in.}} = 1.52 \times 10^7 \text{ lb.}$$

E = Total impact energy

then:

$$L = \frac{1.52 \times 10^7 \text{ lb.}}{2876.7 \text{ in.}^2} = 5{,}283 \text{ psi}$$

Because the load on the concrete is less than its ultimate dynamic load, the integrity of the concrete is protected.

It should be noted that the probability of this postulated accident occurring is extremely low. Two failures must occur before the cask could be dropped. The hoist operator must fail to observe operating procedure and move a cask containing a design basis load over the corner of the shelf while suspended in air above the pool. Then the equipment must fail in such a way that the cask is released. The falling cask must land on the corner of the shelf with its center of gravity directly over the edge. The calculations reflect further conservatism by assuming that the concrete is not reinforced by steel rebar (it is reinforced) and the impact-absorbing pad absorbs all the energy. Also, the fins of the cask will absorb some energy.

A.13.2.5 Fin Weld Analysis

The welding of the fins of the impact pad to the horizontal plates was also analyzed. The static plastic moment of the fin weld (M_p) is given by

$$M_p = \sigma_y \left(\frac{bt^2}{4} \right)$$

where

σ_y = yield stress of 304L (25,000 psi);

b = 1 in. unit length; and

t = fin thickness of 0.5 in.

Then

$$M_p = 25{,}000 \left(\frac{1 \times 0.5^2}{4} \right) = 1{,}560 \text{ psi per unit length of weld}$$

Weld stress (S) is given by:

$$S = \frac{(1.414)M_p}{(b)(L)(h+b)}$$

where

b = 0.25 in., weld size,

h = 0.5 in. fin thickness; and

L = in., weld length.

Then

$$S = \frac{(1.414)\times 1560}{(0.25)(1)(0.5+0.25)} = 11{,}764 \text{ psi}$$

which is less than the yield stress for 304L stainless steel.

This analysis assumes the fin is held firmly by the base plate. The fins will be attached with a fillet weld using 308L stainless steel rods. According to AWS-ASTM classification of corrosion-resisting chromium and chromium-nickel steel welding rods, the tensile strength of 308L stainless steel rod is 75,000 psi. The stress is also less than the permissible stress for welded joints as given in the **Code for Arc and Gas Welding in Building Construction** of the American Welding Society. The permissible shear stress on the section through the throat of a 308L fillet weld is 13,600 psi.

A.13.3 CASK DROP IN DEEP PIT

A.13.3.1 Drop Height and Energy

The fuel unloading pit has been analyzed for a postulated shipping cask drop accident. When a shipping cask is placed in the fuel unloading pit, first the cask is lowered to a shelf 18.5 ft. below the water level. A cask extension yoke is then employed to lower the cask to the unloading pit floor 30 ft. below the step. Assuming the cask is raised 1 ft. above the step surface and then moved horizontally over the unloading pit, the height of the postulated drop is 31 ft. The cask will be underwater during the postulated drop.

The vertical forces acting on the cask (assume downward is the positive direction) are positive gravity, negative buoyancy force and negative drag force. The equations for these forces are:

g = force of gravity = 32.2 ft/sec^2

F_B = buoyancy force = ρV

where

ρ = density of water

V = volume of cask

F_D = drag force = $0.5 C_d \rho \bar{u}^2 A$

where

C_D = drag coefficient = 1.1

ρ = density of water

$\bar{u}$ = average of velocity

A = cross-sectional area of cask

Assuming the cask is a IF-300 shipping cask, acceleration, velocity, drag force, and kinetic energy were calculated in 1 ft. increments throughout the 31 ft. height. The acceleration dropped from 32.2 to 20.5 ft./sec.^{2} due to the drag force, the impact velocity was 38.8 ft./sec. and the kinetic energy was 3,362,484 (4.035 x 10^7 in.-lb.). This energy is less than a postulated 30 ft. drop in air, which is 5.04 x 10^7 in.-lb., and therefore, the consequences will be less than those experienced in a 30 ft. drop in air as far as the shipping cask is concerned.

A.13.3.2 Floor Construction

As indicated in the FSAR (GE document No. NEDO-10178-2, July 1971), the floor of the cask unloading pit rests directly on a shale bed. The ultimate compressive strength of this bed was tested and found to be from 6,000 to 11,000 psi. The floor is made of reinforced concrete 3.83 ft thick and covered with a steel plate 2 in. thick.

A.13.3.3 Floor Loading Analyses

An accidental cask drop in the unloading pit was analyzed for a perpendicular drop and a corner drop. It was found that the corner drop (axis of the cask inclination equal to 14.23°) has the greatest potential for damage to the floor of the unloading pit.

The cask corner drop was analyzed using the modified National Defense Research Committee (NDRC) formula for missile penetration calculations[4]. The analysis was made for the IF-300 shipping cask which weighs 146,000 lb. in air and 126,000 lb. in water, with an impact velocity of 38.8 ft./sec.

A calculation using the modified NDRC formulation showed that the penetration depth is less than 16 in. The foundation mat thickness required to prevent perforation was calculated as 42.3 in. using the NDRC formulation. The total thickness of the concrete floor in the unloading pit is a minimum of 46 in., indicating that there will be no perforation.

The calculations neglect the energy required to deform the cask fins. The total energy of the cask was accounted for in perforation of the steel plate and penetration of the concrete floor. Thus, the penetration is a maximum value.

This analysis did not consider any material below the concrete mat. Since the floor of the unloading pit rests directly on a shale bed, there can be no scabbing of the lower surface of the floor. This adds additional conservatism to the calculation of mat thickness to prevent perforation and thus to the conclusion that no perforation of the concrete mat will occur.

Since perforation of the concrete floor is not expected, the only consequence of a cask drop accident would be penetration of the pit liner with release of small quantities of basin water to the region between the liner and concrete wall. Experience at GEH-MO with a cask tipping incident[5] has shown that leakage due to a breach of the pit liner can be handled with no measurable release of basin water from the facility to the local perched aquifers and liner repair can be made in a short time with no serious impact on the operation of the fuel storage facility.

According to R. P. Kennedy (Reference 4) the modified NDRC formula is applicable to this case since it adequately predicts test results for large-diameter, low-velocity missiles.

Even if the results of the penetration/perforation analysis are ignored and it is very conservatively assumed that the corner cask drop results in a breach of the concrete mat such that there is leakage of pool water to the local perched aquifers; there would be no significant release of radioactivity to accessible water sources.

Analyses of the leakage paths of water from the fuel basin is contained in Dames & Moore's, "Transport Modeling for Accidentally Released Water from Spent Fuel Storage Basin at Morris, Illinois Facility of General Electric Company", October 26, 1993.

A.13.4. REFERENCES

1. D. Hartog, "Flat Plate Theory," **Advanced Strength of Materials.**

2. Atchley and Furr, "Strength and Energy Absorption Capacities of Plain Concrete Under Dynamic and Static Loading," **ACI Journal**, November 1967. **Discussions,** 65: 414-16, May 1968.

3. **Loading Pit Concrete Tests**, by H. H. Holmes Testing Lab., Inc., April 1969, under AE Contract No. 4204.

4. R. P. Kennedy, **A Review of Procedures for the Analysis and Design of Concrete Structures to Resist Missile Impact Effects,** Nuclear Engineering and Design, Volume 37, 1976 pp. 183-203.

5. B. F. Judson, Plant Manager, General Electric Co., MFRP, Morris, Illinois, letter to B. Grier, Regional Director, USAEC, Division of Compliance - Region III, 799 Roosevelt Road, Glen Ellyn, Illinois, June 27, 1972.

A.14 LIST OF ENGINEERING DRAWINGS

Figure	Title
A.14-1	Main Building Below Elevation 45' 0" and 48' 0"
A.14-2	Main Building - Sections A, B, J, K and L
A.14-3	Main Building - Sections E and F
A.14-4	Main Building - Longitudinal Section G
A.14-5	Main Building - Longitudinal Section H
A.14-6	Sand Filter Building - Floor Plan
A.14-7	Sand Filter Building - Isometric

Drawing	Title
C5483E-2351	Grid Assembly Detail 'J.'
V3874 17988-D	Basket Ass'y BWR Fuel
V3887 17987-D	Basket Ass'y PWR Fuel
C6221 17988-E	Basket Ass'y BWR Fuel - Square Tube Design

Figure A.14-2 Main Building Below El. 45' 0" and 48' 0"

Figure A.14-2, Main Building Sections A, B, J, K, & L

Figure A.14-3, Main Building – Section E and F

Figure A.14-4, Main Building – Longitudinal Section G

Figure A.14-5, Main Building – Longitudinal Section H

Figure A.14-6 Sand Filter Building – Floor Plan

Figure A.14-7 Sand Filter Isometric

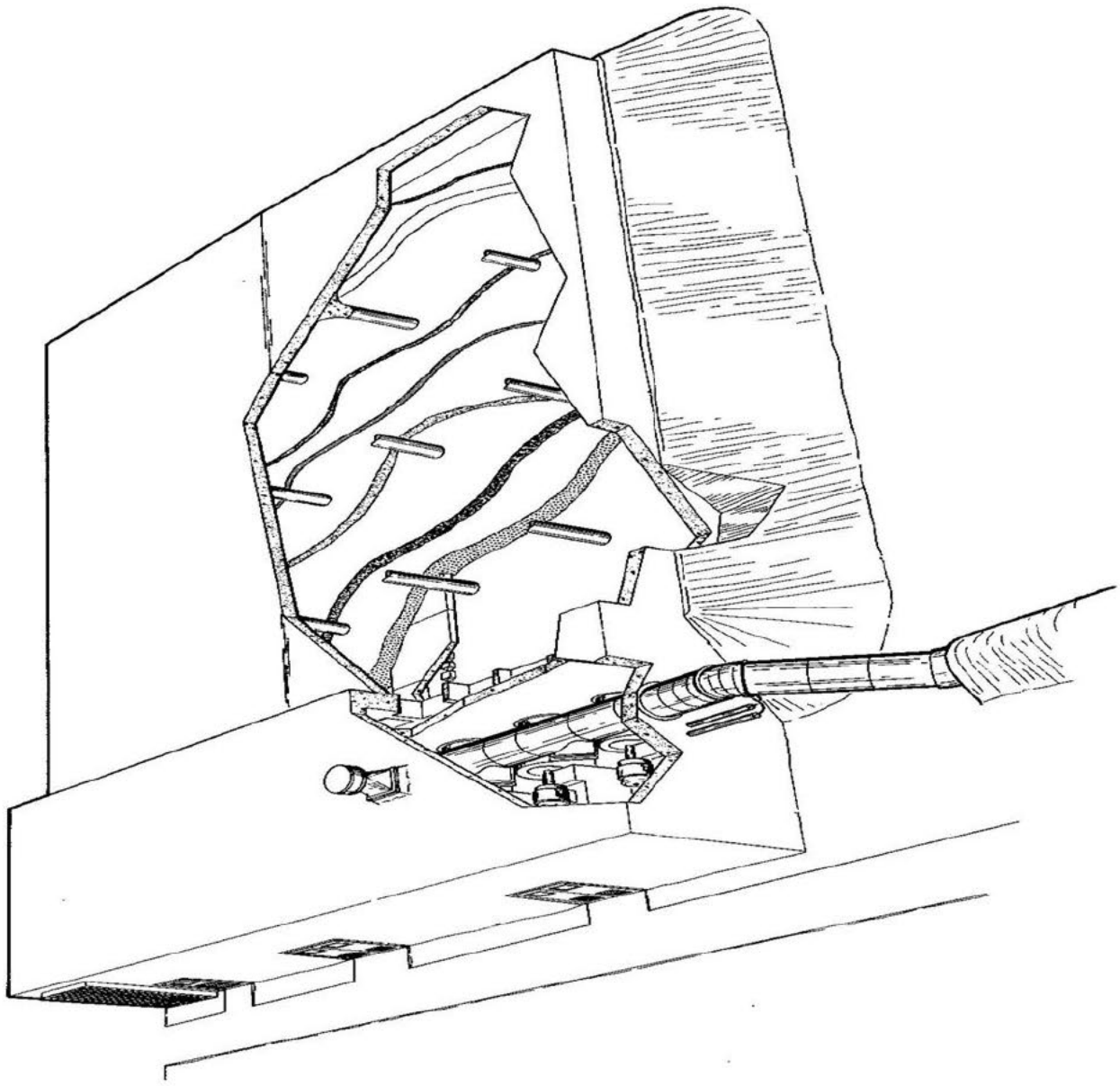

Drawing C5483-2351 Grid Assembly Detail 'J'

[redacted]

Drawing V3874 17988-D

Drawing V3887 17987-D

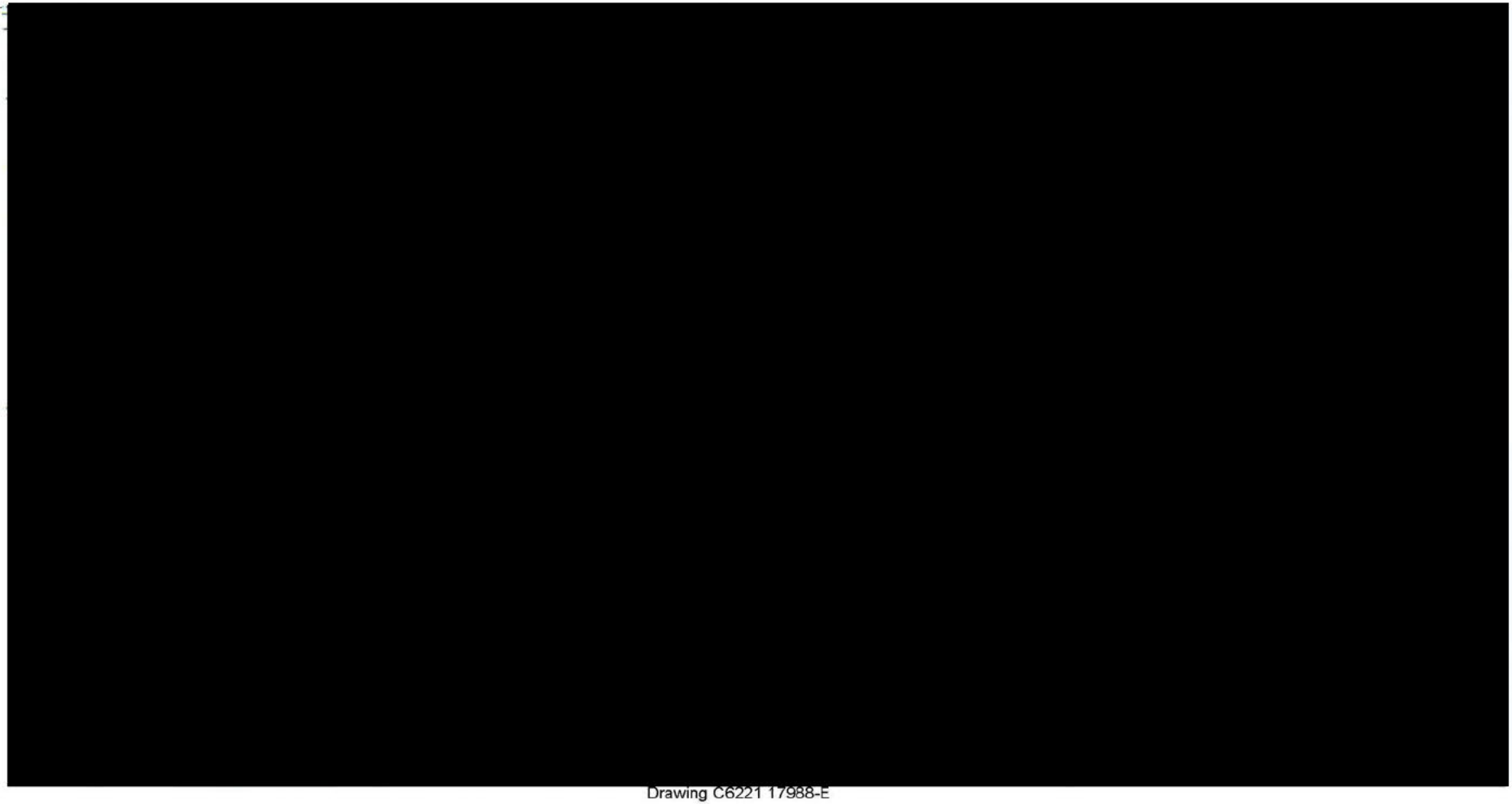

Drawing C6221 17988-E

A.15 ANALYSIS OF TORNADO MISSILE GENERATION AND IMPACT ON THE MORRIS OPERATION FUEL STORAGE BASIN

A.15.1 INTRODUCTION

Only those windborne objects, which could have a significant downward velocity on entry into the water-filled basin, have the potential for causing damage to basin contents. Such objects must have been at a significant elevation above ground level, prior to entry, to develop the required vertical velocity component to result in damage.

A.15.2 POTENTIAL MISSILES

Potential missiles can be classified in regard to their relative elevation, as follows:

1. Objects in the immediate area which, when the tornado strikes, are at elevations above the level of the basin surface (operating equipment and auxiliaries, components of the enclosing structure, etc.).

2. Objects in the general vicinity, which are of such shape and density that they become airborne by aerodynamic lift, are carried by the tornado for a distance and then are dropped into the basin (roofs, doors, etc.).

3. Objects in the general vicinity which are too heavy to be lifted by aerodynamic forces, but which conceivably could be deflected upward into a ballistic trajectory after being accelerated by the tornado winds at ground level (small automobiles, boulders, etc.)

4. Objects in the general vicinity, which are too heavy to be lifted but, when the tornado strikes, are already at a location above ground level (tops of telephone poles, etc.) so that they could be carried by the tornado and dropped into the basin.

Fuel handling tools and equipment, as well as building siding and roof decking, are of low mass and could not be accelerated over the distance required to achieve the potential velocity at which damage could occur, since they are located within the immediate vicinity of the basins. Heavier items, such as fuel shipping casks, are capable of withstanding tornado winds without displacement.

To become airborne by aerodynamic lift, objects in the second category must be relatively light and of large surface area. Thus, high impact velocities would be required to cause damage, but deceleration would be rapid upon entry into the water. For these reasons, damage potential from such objects is not significant.

Although the likelihood of actual occurrence is very low, objects in the third category must be considered because they are relatively dense and conceivably could arrive at the basin location with a high downward velocity.

Objects in the fourth category do not have significant damage potential because of their limited initial elevation, except as they may be deflected upward, after initial acceleration, in which case they become similar to the missiles described in the third category. In summary, only dense objects, which achieve significant elevations by the mechanism described for the third category appear to have potential for inflicting damage to the basins or fuel.

In recognition of the fact that sufficient data are not available on which exact characterization can be based, four different methods of calculating potential missile velocities are considered. Three of these are derived from sources in the literature and the fourth from discussions with U. S. Weather Bureau Personnel. These methods are then applied to two simple geometrical bodies typical of potentially damaging missile objects, as described above; viz., a 12 in. diameter by 20 ft. long section of telephone pole weighing 630 lb. and a small automobile, 5 ft. by 5 ft. by 8 ft. in dimension and weighing 1,800 lb.[1]. The most conservative conditions of acceleration and ramp deflection are used in evaluating potential missile effects, although the analysis is based on assumptions regarding missile behavior, which have a very low probability of actual occurrence.

A.15.3 TORNADO WIND VELOCITIES

A tornado is a violent whirlwind usually accompanied by a funnel cloud produced by low pressure inside the storm. Estimates of wind speed within the tornado funnel have been made directly from the shape of the funnel cloud, moving and still pictures of funnels and debris, and the extent of damage and patterns on the ground resulting from flying debris. Estimates of tangential wind speeds from damage can be significantly in error due to the many assumptions, which must be made. Studies by Fujita, et. al. indicate that minimum wind speeds ranging from 55 to 217 mph are required to effect the typical damage wrought by Midwestern tornadoes.

Measurements of the Fargo tornadoes show a maximum tangential wind speed of about 230 mph with a translational speed of about 30 mph. The Dallas tornado measurements show a maximum tangential velocity of 170 mph and an average translational speed of 27 mph. Goldman calculated vertical velocities of 126 mph at a 750 ft. radius and about 900 ft. above the ground in studies of the Illinois tornadoes of April 1963. The tangential speed along the funnel edge of a Texas tornado of March 1956 was computed as about 230 mph at a radius of 200 ft. and 2,700 ft. above the ground. Some old estimates of 500 mph have been largely discounted over the last few years as more knowledge has been compiled on the subject, and it can be concluded that a maximum tangential speed of 300 mph is a conservative speed to be used in design of nuclear power facilities[2].

A.15.4 ANALYTICAL CRITERIA

The analyses reported herein were based on the following criteria:

Maximum Wind Velocity - 300 mph

Missile No. 1 Telephone pole, 12 in. diameter x 20 ft., weight assumed as 40 lb./ft.^{3}

Missile No. 2 Small automobile, 5 ft. x 5 ft. x 8 ft. long, weight assumed as 1,800 lb.

Drag Coefficient1.3

A.15.5 ANALYTICAL METHODS

In several of the analysis methods used the trajectory of the missiles is considered, while in other methods the energy produced in the missile is translated to velocity or height and combinations of both.

For an object to become a missile, it is necessary for it to be aerodynamically lifted and set in motion by the winds of the tornado. The three modes of injection are:

a. Explosive injection into the suddenly imposed pressure differential of the tornado. Here there must be a sufficient volume of air below the object injected to cause the explosion (for example, roofs on poorly vented building).

b. Aerodynamic injection of an object having some configuration which produces lift in the horizontal flow.

c. Ramp injection, where the object is accelerated horizontally and deflected upward.

Aerodynamically, it is impossible for a 300-mph wind to generate missiles approaching that speed because the object has to be accelerated and is subject to the influence of its shape, weight and friction relative to the air.

Four methods are used to determine the speed of the missiles under consideration. Method 1 assumes the object is accelerated and deflected upward at an angle of 45° while constantly exposing a maximum area perpendicular to the direction of the wind. Method 2 is similar to Method 1 in that the distance through which it is acted upon and the manner of acceleration are the same, but the object is considered to tumble as it travels with the tornado winds. In Method 3, an initial elevation is assumed, and the missile is acted upon by simultaneous horizontal and vertical wind forces. In Method 4, a tumbling object is acted upon by the maximum winds over an average period of time.

A.15.5.1 Method 1

The following assumptions are made in this procedure[2]:

a. The velocity of the tornado winds at ground level is 300 mph.

b. The force associated with a 300 mph tornado acts on the object over a horizontal distance equal to a 90° chord of the diameter of the maximum velocity of the tornado. The linear horizontal distance (the chord) from the point at which the tornado picks up the object, to the point where it leaves the tornado, is 348 ft.

c. The maximum area of the missile remains perpendicular to the winds for the entire distance over which it is accelerated.

d. The object is deflected upward at an angle of 45° without loss of energy.

e. No drag force acts on the object once it leaves the tornado.

Horizontal acceleration may be expressed as:

$$\ddot{X}\left(\frac{W}{g}\right) = \frac{C_d A_m d\left(V_w - \dot{X}\right)^2}{2g}$$

and

$$\ddot{X} = \frac{C_d A_m d\left(V_w - \dot{X}\right)^2}{2W}$$

where

C_d = drag coefficient

A_m = maximum cross-sectional area of the object

d = density of air

V_w = wind velocity

$\dot{X}$ = horizontal velocity of object

W = weight of object

This equation can be solved for $\dot{X}$ as expressed in the following form:

$$\frac{V_W}{\left(V_W - \dot{X}\right)} - \log_e\left(V_W - \dot{X}\right) = \left(C_d A_m d\left(\frac{X}{2W}\right)\right) + 1$$

where X is the chord distance described in assumption b., above, Once the object has left the tornado area, it is acted upon by gravity only. The equations of motion are:

$$Y = \left(\frac{-gt^2}{2}\right) + \dot{X}_0 \sin 45° t$$

$$\dot{Y} = -gt + \dot{X}_0 \sin 45°$$

$$X = \dot{X}_0 \sin 45° t$$

$\dot{X} = \text{constant} = \dot{X}_0 \sin 45° =$ horizontal velocity after the object is deflected 45° upward

$\dot{X}_0 =$ horizontal velocity of object when leaving tornado

The vertical and horizontal velocities and displacements of the missile after it has left the tornado may be calculated using $\dot{X}_0$ and $\dot{X}_0 \sin 45°$ as initial conditions.

Several assumptions for this method are very conservative. A tangential wind velocity of 300 mph is a conservative maximum value and is common design practice[2]. Furthermore, maximum winds normally occur better than 100 ft. above the ground, so that a ground level assumption is very conservative. The distance over which the object is acted upon by maximum winds is also conservative. Since the momentum of the object will cause it to be hurled in a straight line, the distance over which an object would be accelerated by winds would necessarily be limited to something less than the assumed 90° chord. Furthermore, the object would most certainly bounce several times, thereby slowing the missile down. The assumption that the maximum area of the missile remains perpendicular to the winds for the entire distance over which it is accelerated is very conservative. Some objects, such as roofs and trees, can sail and soar in the winds, but objects which present the most serious potential hazards to the fuel in storage are not aerodynamically stable, and will turn in the wind.

A.15.5.2 Method 2

Method 1 assumes that the maximum area of an object remains constantly perpendicular to the wind. Method 2 is largely predicated on the same assumption as is Method 1, except the object

is assumed to tumble in the wind, and its energy may be expressed as velocity or height or combinations of both. The force exerted by wind on an object is expressed as:

$$D_f = 0.5 C_d d \left(V_w - \dot{X}\right)^2 \left(A_+ \cos^2 a + A_= \sin^2 a\right)$$

where a is the angle of the wind with respect to an orthogonal axis of the object, A_+ is the cross-sectional area perpendicular to the wind, and $A_=$ is the cross-sectional area parallel to the wind.

Most frequently, the object tumbles in such a manner that the wind makes a random angle with respect to the orthogonal axes. The average values of $\cos^2 a$ and $\sin^2 a$ are therefore 1/4, obtained by squaring their values integrated over all angles from 0 to π, and the equation becomes:

$$F_{ave} = 0.125 C_d d \left(V_w - \dot{X}\right)^2 \left(A_+ + A_=\right)$$

Very short increments of time are used to determine the velocity of the object at any instant:

$$\dot{X}_i = \dot{X}_{i-1} + F_{ave} / M(dt)$$

A step-by-step integration is then used to determine the final velocity.

A.15.5.3 Method 3

This method was presented by Bates and Swanson[3], and later included in a paper by Doan[4]. As in the previous method, tumbling of the object is assumed. The average force on the object is assumed to act for an average time of application, and the difference in velocities between the wind and the missile is not considered. The force acting on the object is approximately:

$$F_d = q\, C_d \left(A_+ \cos^2 a + A_= \sin^2 a\right)$$

where:

$$q = 1/2\, d\, V_w^2$$

Again, the values of $\cos^2 a$ and $\sin^2 a$ are determined to be 1/4, and the equation becomes:

$$F_{ave} = 1/4\, C_d\, q \left(A_+ + A_=\right)$$

The speed and kinetic energy of the missile are:

$$\dot{X} = F_{ave} t_{ave} / M$$

$$E = F_{ave}^2 t_{ave}^2 / 2M$$

where t_{ave} is the average time of force application. This average is estimated to be on the order of 0.2 second.

If all of the energy acquired is used to lift the object vertically, the maximum height attained is:

$$H_{\max} = \frac{F_{ave}^2 t_{ave}^2}{2Mg}$$

Bates and Swanson observe that the force exerted on a fixed object (conserved angle of attack) is of short duration because by the time the aerodynamic force has increased to a value sufficient to lift most objects, the moments which produce tumbling are also large. The mean time interval of action is estimated as 0.2 second. Doan does not discuss the merits of his time interval for a tumbling object, but simply estimates it as 0.2 second. The relatively low values obtained from this method reflects this short period of time.

A.15.5.4 Method 4

This method was developed after discussions by telephone with several offices of the Weather Bureau concerned with tornadoes and is based on the following assumptions:

a. The object is acted upon by the maximum winds for a distance equal to the radius of the tornado.

b. A maximum horizontal wind of 300 mph and a maximum vertical wind of 300 sin 45° mph act constantly on the vertical and horizontal faces of the object.

c. Since vertical velocities are small at the ground surface, it is assumed that the object is initially at a height of 30 feet above the ground.

The two basic equations of motion for objects within the tornado are:

$$M\ddot{Y}_1 = F_y - Mg$$

$$M\ddot{X}_1 = F_x$$

where $\ddot{Y}_1$ and $\ddot{X}_1$ are the accelerations within the tornado; F_y and F_x are the forces due to the tornado-induced pressures in the vertical and horizontal directions, respectively. The initial

motion of the object when encountered by the tornado is zero. Upon leaving the tornado area, the missile is acted upon by gravitational force alone, and the equations become:

$$M\ddot{Y}_2 = -Mg$$

$$M\ddot{X}_2 = 0$$

Here, the initial velocity conditions are the maximum attained within the tornado.

A.15.6 Discussion and Results

Results of these analyses are listed in Table A.15-1 and applied in Section 8. Method 1 proved the most severe, the second being Method 2. Principal differences of all of the methods are: a. constant exposure of maximum missile area to wind versus a tumbling action, and b. the duration of time of wind acting on object. While the time element of Method 3 or 4 may be more nearly correct, the lack of pertinent information on the effective time of attack rules in favor of Methods 1 and 2. Of these, method 2 is more realistic but impact analyses were performed for velocities calculated by Method 1 to be more conservative.

Table A.15-1
RESULTS OF WIND ANALYSES

Missile	Telephone Pole 12-in. Diameter x 20 in. (630 lb)				Automobile 5 ft x 5 ft x 8 ft long (1,800 lb)			
	Maximum Velocity (ft/sec)		Maximum Distance (feet)		Maximum Velocity (ft/sec)		Maximum Distance (feet)	
	Horizontal	Vertical	Horizontal	Vertical	Horizontal	Vertical	Horizontal	Vertical
Method 1	264[a]	187	2174	543	242[a]	171	1820	455
Method 2	171[a]	121	899	228	187[a]	132	1083	271
Method 3	16	-	6	4	17.5	-	7	5
Method 4	71	53.5	195	44	49	50.5	112	36

a Horizontal velocity before the object is deflected upward at 45°

A.15.6.1 Impact Analysis

For analysis of impact effect within the water-filled basins, it is further assumed that the object enters the water vertically at the velocities calculated from the above assumptions (187 ft./sec. for the telephone pole and 171 ft./sec. for the automobile), as shown in Table A.15-1, in an "end on" orientation.

Upon entering the basin water, forces acting on a missile are:

(1) Mass inertia $(m\dot{x})$

(2) Weight of the missile (mg)

(3) Buoyancy (ρvg)

(4) Drag $\left(\frac{C_d A\dot{x}^2}{2}\right)$

where:

m = mass of the missile

v = submerged volume of the missile

A = area of the missile perpendicular to the direction of movement

C_d = drag coefficient (assumed in all cased to be 1.0)

$\ddot{x}$ = missile acceleration at time t

$\dot{x}$ = missile velocity at time t

ρ = mass per unit volume of the basin water

For passage of a missile through the basin water,

$$m\ddot{x} = mg - \left(\frac{C_d A\dot{x}^2}{2}\right) - \rho vg,$$

or

$$\ddot{x} = g - \left(\frac{C_d A \dot{x}^2}{2m}\right) - \frac{\rho v g}{m} = \left(1 - \frac{\rho v}{m}\right) - \left(\frac{C_d A}{2m}\right)\dot{x}^2,$$

and

$$\ddot{x} = \frac{d\dot{x}}{dt} = \left(\frac{d\dot{x}}{dx}\right)\left(\frac{dx}{dt}\right) = \frac{\dot{x}d\dot{x}}{dx}$$

Letting $\theta = C_dA/m$ and $\phi = g\,(1 - \rho v/m)$ and noting that $\dot{x} = V_0$ at $x = 0$,

$$\dot{x}^2 = \frac{2\phi}{\theta} + \left(V_0^2 - \frac{2\phi}{\theta}\right)e^{-\theta x}$$

In the case of the telephone pole, a step-by-step solution was developed to evaluate its velocity at different depths of penetration, assuming constant end-on orientation. On this basis, velocity after penetrating to a depth of 8 ft. is 138 ft./sec.; after 14 ft., 111 ft./sec.; and after 21 ft., 88 ft./sec.. Total penetration required to stop the pole exceeded the depth of the basin. On striking the bottom liner, missile kinetic energy would be approximately 5×10^4 ft.-lb.

For the automobile, no buoyancy was assumed until after it had penetrated 2 ft. into the basin water and its submerged volume then was assumed to remain constant to account for leaks. On this basis, total penetration for deceleration to terminal velocity (< 6 ft./sec.) was 7.3 ft.

A.15.6.2 Effects of Missile Impact on Basin Structure

The potential penetration of the basin liners and wall by the postulated missiles was evaluated[5]. The penetration of a steel plate is described by the equation:

$$\frac{E}{D} = U\left(0.344t^2 + 0.00806wt\right)$$

where:

E = critical kinetic energy required for penetration;

D = diameter of missile (in.);

U = ultimate tensile strength of steel;

t = thickness of steel plate (in.); and

w = distance between supports of the plate (in.).

The penetration and perforation of concrete, masonry and sand is similarly described by the equation:

$$D' = KAV'R$$

where

D' = depth of penetration (ft);

K = penetration coefficient for reinforced concrete = 4.76 ft./lb.;

A = sectional mass of missile (lb./ft.^{3});

R = thickness ratio of the penetration of a slab of thickness T to the penetration of a slab of infinite thickness;

V' = velocity factor for impact penetration = $\log_{10}\left[1+\frac{V^2}{215{,}000}\right]$

where:

V = missile velocity.

Material properties and structural dimensions used in the analysis were:

t = 0.125 in. for basin liners up to 16 ft. elevation

= 0.0625 in. for basin liners above 10 ft. elevation

= 2 in. for deep pit floor

U = 75,000 psi (70,000 for deep pit)

D (telephone pole) = 13.5 in. diameter

D (small automobile) = 61.2 in. diameter

W = 3 ft.

Analyses were performed, for each postulated missile, for potential penetration of each type of material (i.e., assuming no concrete backing for the steel plate and for concrete penetration assuming no liner). Both the walls and floor of the basin were analyzed for potential penetration.

A.15.6.3 Analysis

Wood planks, sections of steel pipe, a telephone pole and a small automobile have been analyzed as potential missiles. Of these missiles, the telephone pole and the automobile represent equivalent or greater potential damage than the others. The analysis of the automobile missile indicates that it does not have sufficient energy to penetrate the 1/16 in. thick wall liner even at its maximum horizontal velocity of 440 ft./sec. due to the large impact cross-sectional area of the automobile. At the maximum horizontal velocity, the kinetic energy of the automobile (5.4×10^6 ft.-lb.), ignoring the fact that the liner is backed by reinforced concrete. The automobile would be traveling in a trajectory and thus would not strike the wall perpendicularly. There is no possibility of penetrating the 3/16 in. thick floor liner as the automobile would be traveling at its settling velocity (< 6 fps) and the kinetic energy is only, about 1,000 ft.-lb.

The analysis of the impact of the telephone pole missile indicates that puncture of the basin liner is extremely improbable. For example, the energy required to penetrate the floor liner in the basin, ignoring the backup strength of the concrete, is in excess of 1.6×10^6 ft.-lb. for an impact perpendicular to the liner. At that depth, the kinetic energy of the telephone pole is less than 5×10^4 ft.-lb., and, thus, there will be no penetration of the floor liner in the basins. A recent report[6] indicates that telephone poles (utility poles) are ineffective in producing significant local and structural damage even under the most improbable missile impact conditions.

The telephone pole cannot strike the walls at any angle that is nearly perpendicular at a depth sufficient to cause significant leakage even if the liner should be penetrated. Penetration of the liner near the top of the pool would not be of concern and penetration of a vertical wall deep in the pool would require more energy than bottom penetration (1.6×10^6 ft.-lb.) due to the angle of impact. For example, after travel through 21 ft. of water, the impact kinetic energy would be only about 4.29×10^5 ft.-lb. Even for a perpendicular impact, penetration can occur only if the concrete backing is ignored. The compressive strength of the concrete might be exceeded in

local areas, but due to the low void fraction of structural concrete and its confinement, there would be no significant crushing. Therefore, the telephone pole will not penetrate the wall liners based on the strength and ductility of the liner, on the possible angle of impact, and on the relative crushing strengths of the pole and the concrete.

It is concluded that penetrations of the basin liners caused by the telephone pole missile are very unlikely and that the leaks resulting from such penetrations, if any, are well within the repair capability of GEH-MO.

A.15.7 REFERENCES

1. Other postulated missiles (pipe, wood planks, steel rod, etc.) have less damage potential than those missiles considered.

2. D. R. Miller and W. A. Williams, Tornado Protection for the Spent Fuel Storage Pool, General Electric Company, November 1968 (APED-5696).

3. F. C. Bates and A. E. Swanson, Tornado Design Considerations for Nuclear Power Plants, Black & Veatch, Engineers

4. P. L. Doan, Tornadoes and Tornado Effect Considerations for Nuclear Power Plant Structures including the Spent Fuel, United Engineers and Constructors.

5. C. V. Moore, Design of Barricades for Hazardous Pressure Systems, Nuclear Engineering and Design (1967).

6. Sandia Laboratories, Full-Scale Tornado-Missile Impact Tests, July 1977 Electric Power Research Institute Report No. EPRI NP-440.

A.16 STRUCTURAL EVALUATION OF MORRIS EXPANSION GATE #4 FOR SPENT FUEL STORAGE BASIN

A.16.1 INTRODUCTION

Consequent to the Nuclear Regulatory Commission (NRC) inspection (NRC Inspection Report No. 072-00001/11-01 (DNMS) – General Electric-Hitachi Morris, dated May 13, 2011), it was discovered that design basis calculations for gate number 4 of the spent fuel pool were not available. The analysis has been conducted and the purpose of this appendix is to provide the details of the calculations that were used to determine that no modification to expansion gate number 4 is required.

A.16.2 ATTACHMENTS

Attachment 1 Engineering Calculation Sheet Number: eDRF Section 0000-0137-7338 REV. 1 (eIV 0000-0148-6891) dated June 1, 2012.

Attachment 1

HITACHI GEH PROPRIETARY INFORMATION *Engineering Calculation Sheet*

[redacted]

HITACHI GEH PROPRIETARY INFORMATION *Engineering Calculation Sheet*

HITACHI GEH PROPRIETARY INFORMATION *Engineering Calculation Sheet*

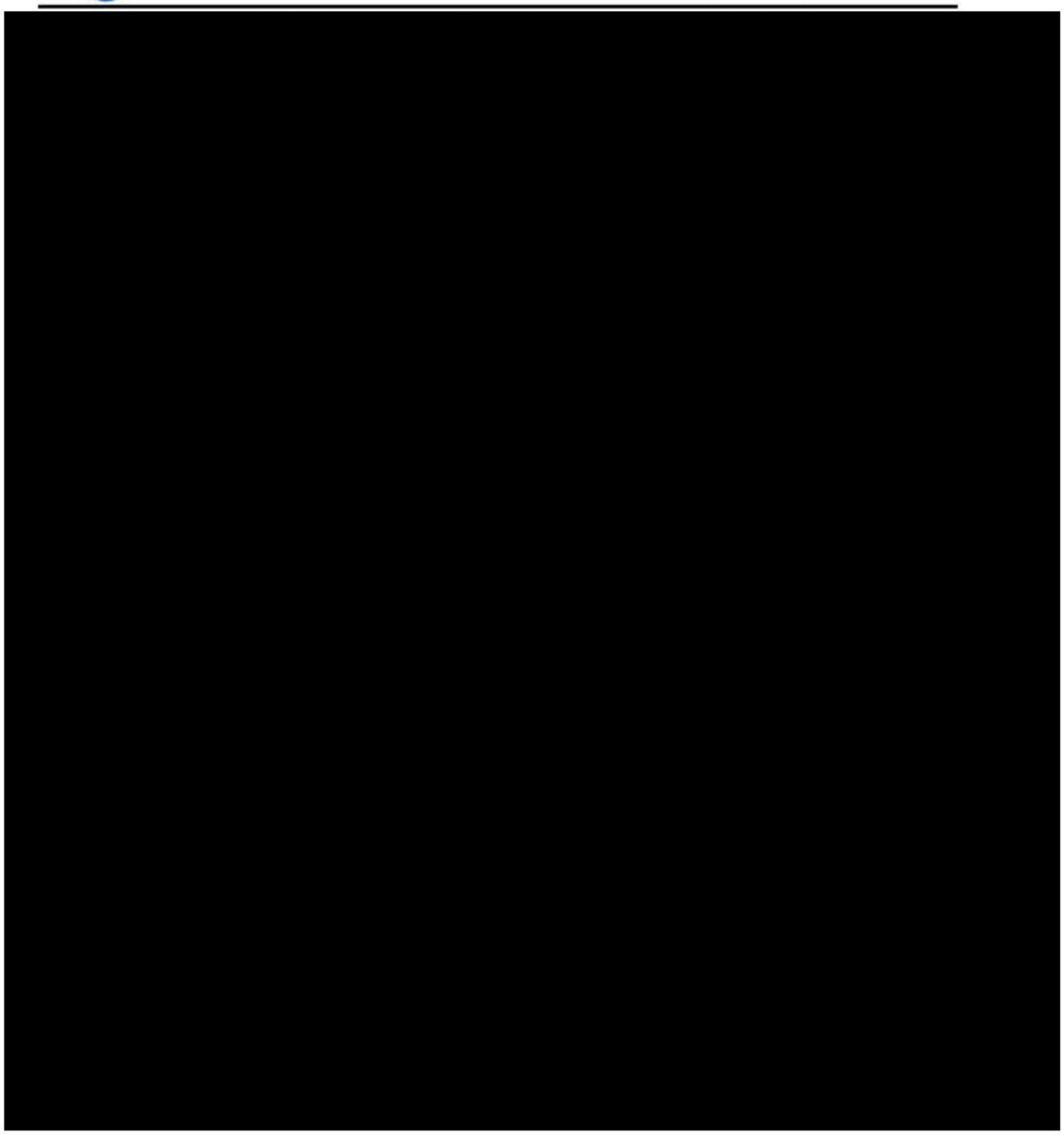

HITACHI GEH PROPRIETARY INFORMATION *Engineering Calculation Sheet*

HITACHI GEH PROPRIETARY INFORMATION *Engineering Calculation Sheet*

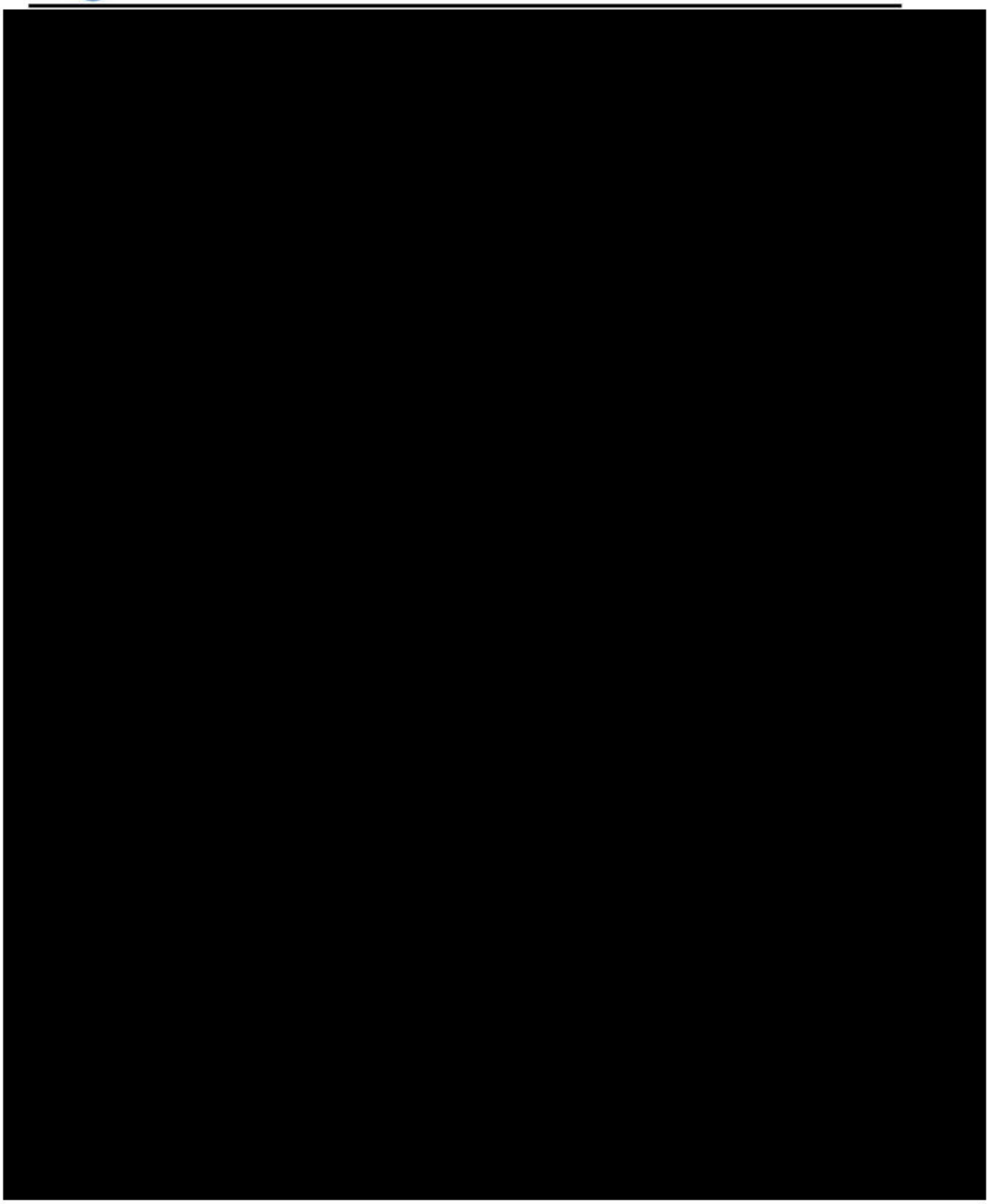

HITACHI GEH PROPRIETARY INFORMATION *Engineering Calculation Sheet*

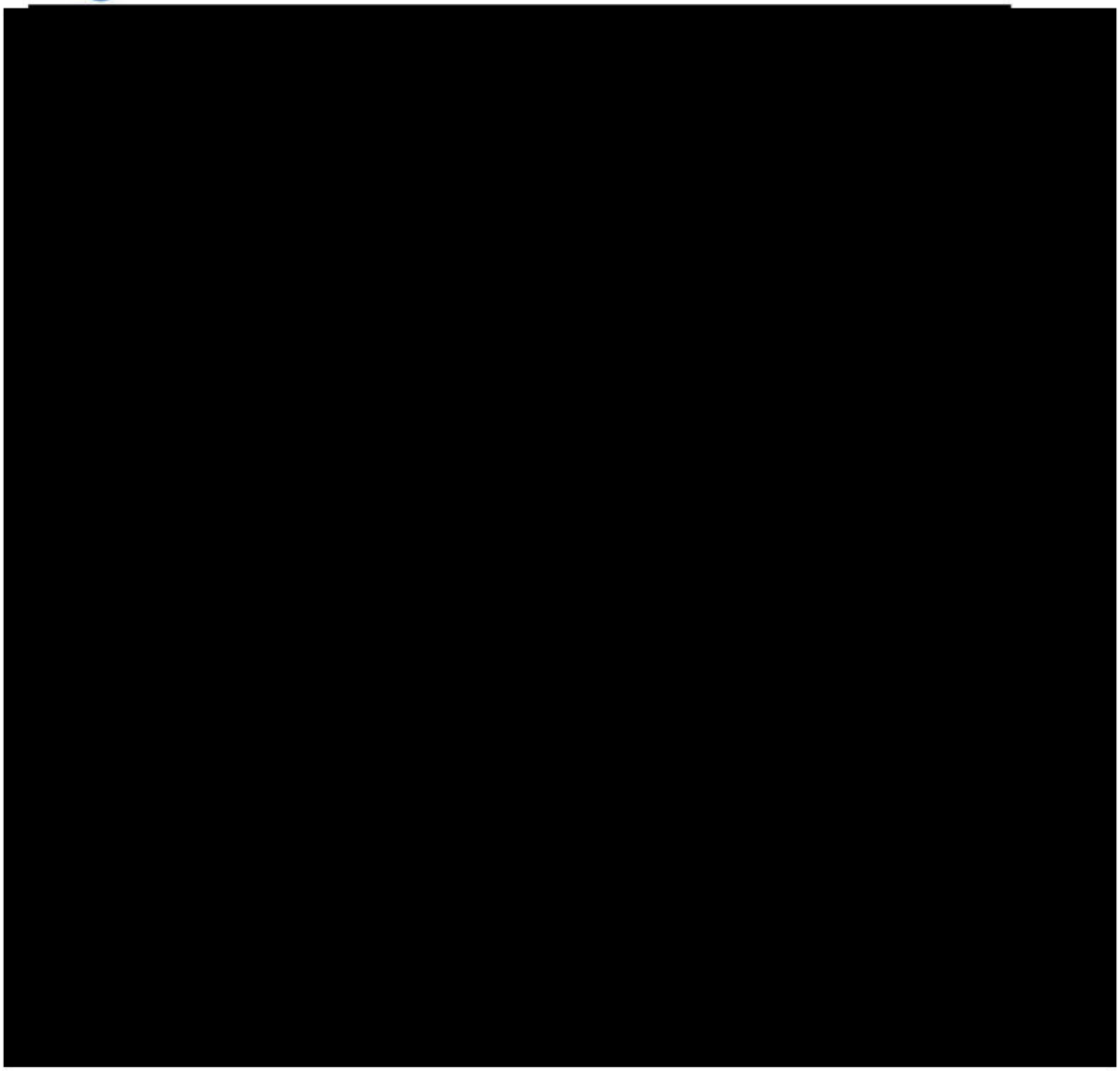

HITACHI GEH PROPRIETARY INFORMATION *Engineering Calculation Sheet*

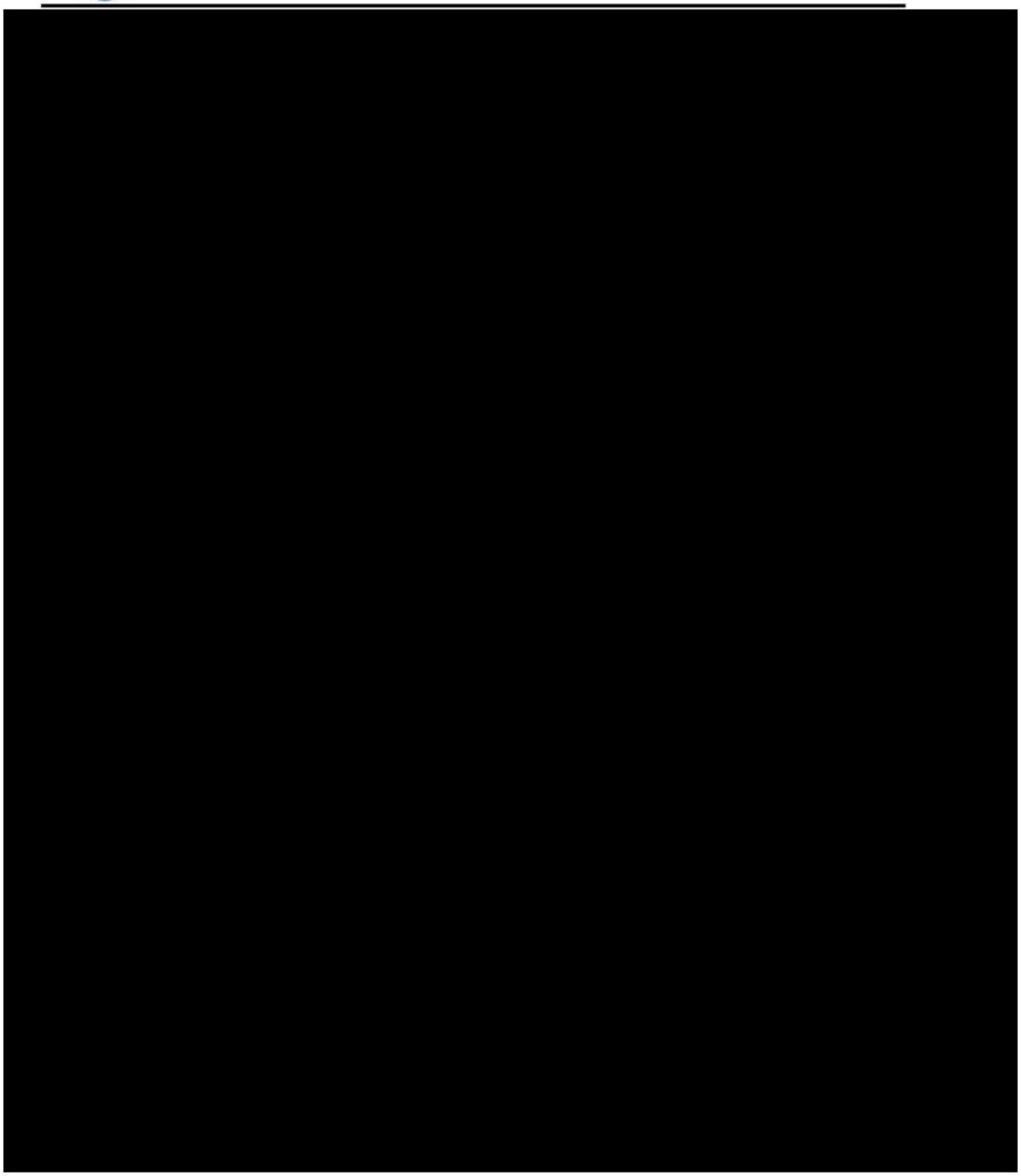

HITACHI GEH PROPRIETARY INFORMATION *Engineering Calculation Sheet*

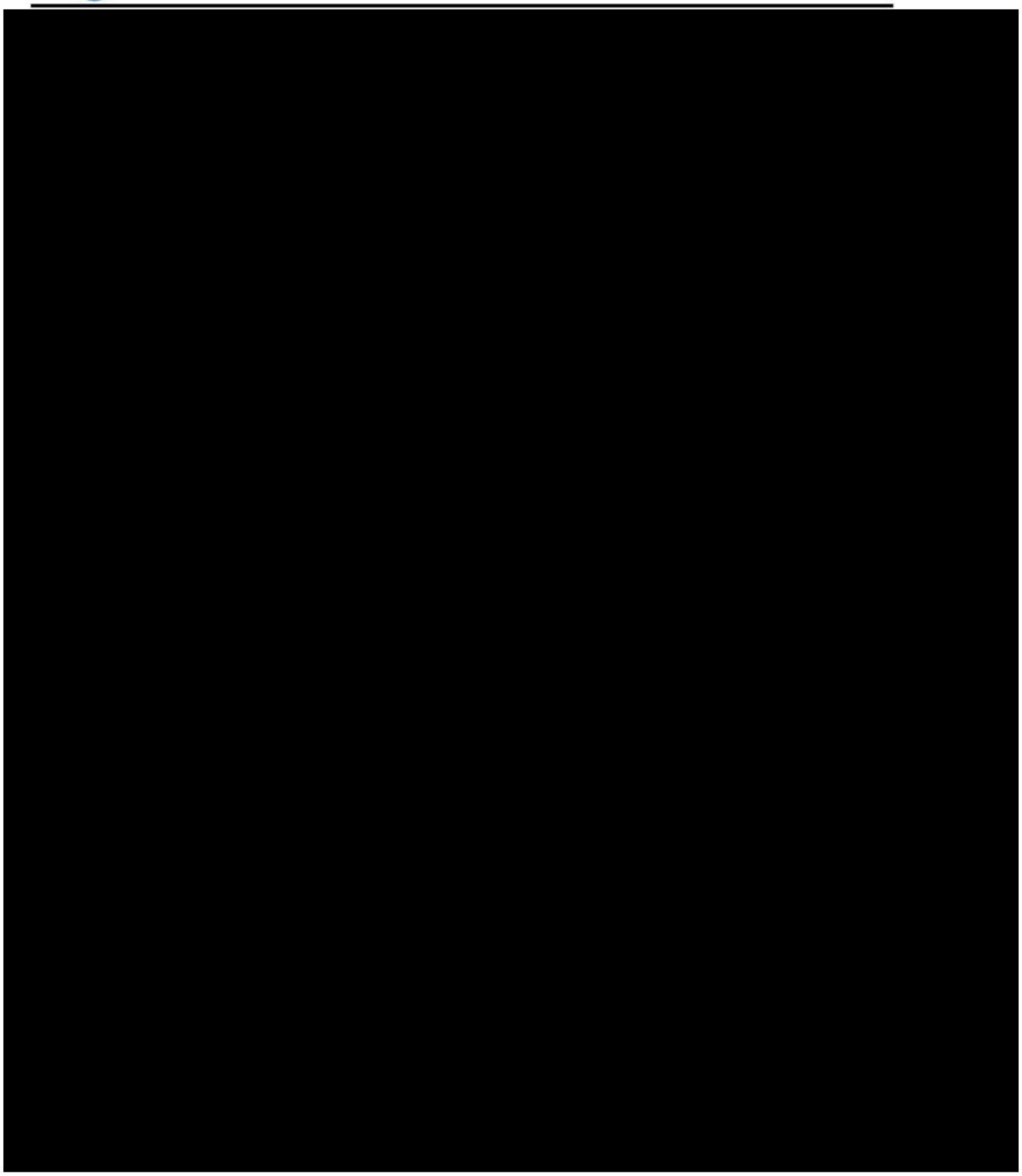

HITACHI GEH PROPRIETARY INFORMATION *Engineering Calculation Sheet*

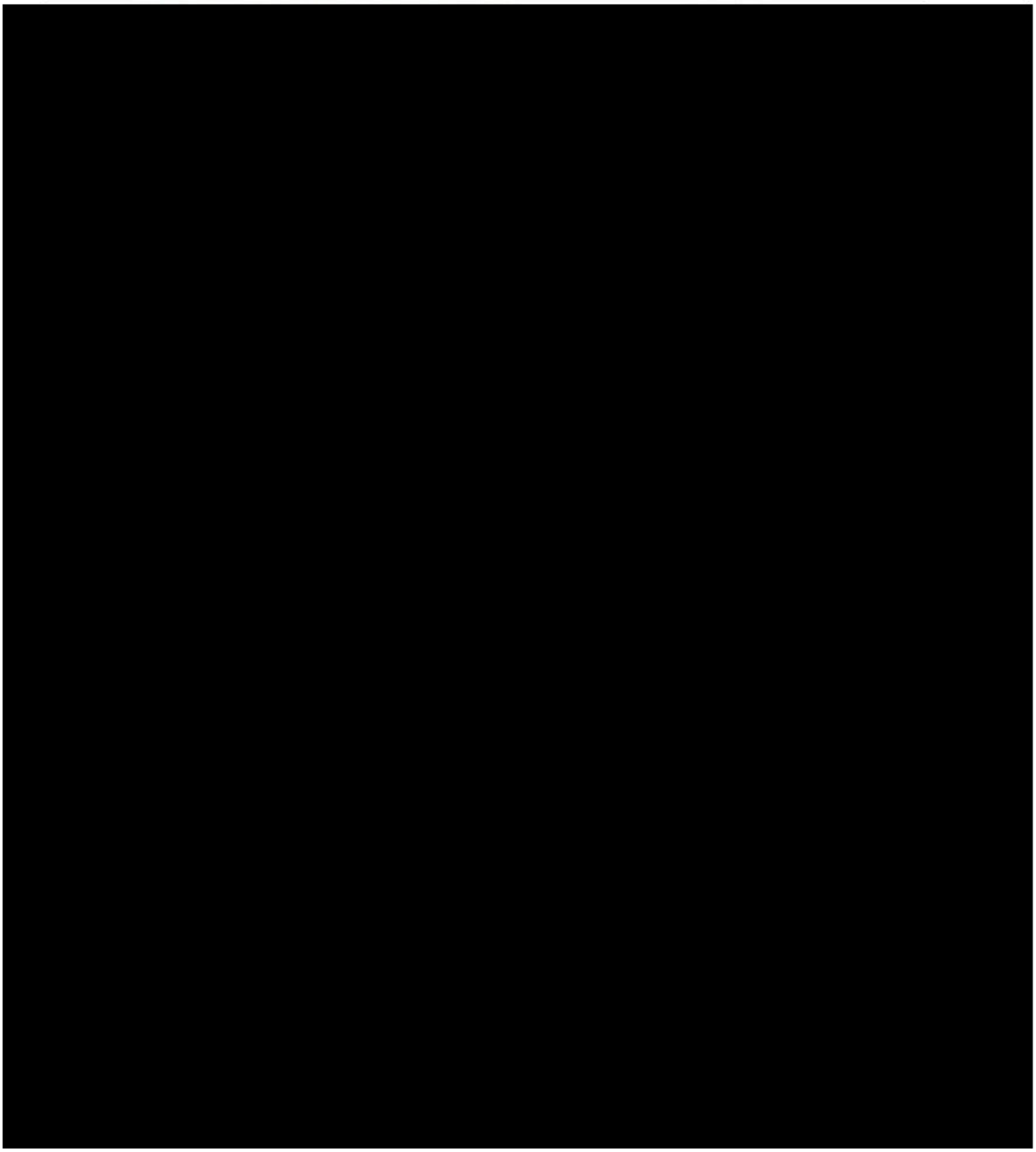

HITACHI GEH PROPRIETARY INFORMATION *Engineering Calculation Sheet*

HITACHI GEH PROPRIETARY INFORMATION *Engineering Calculation Sheet*

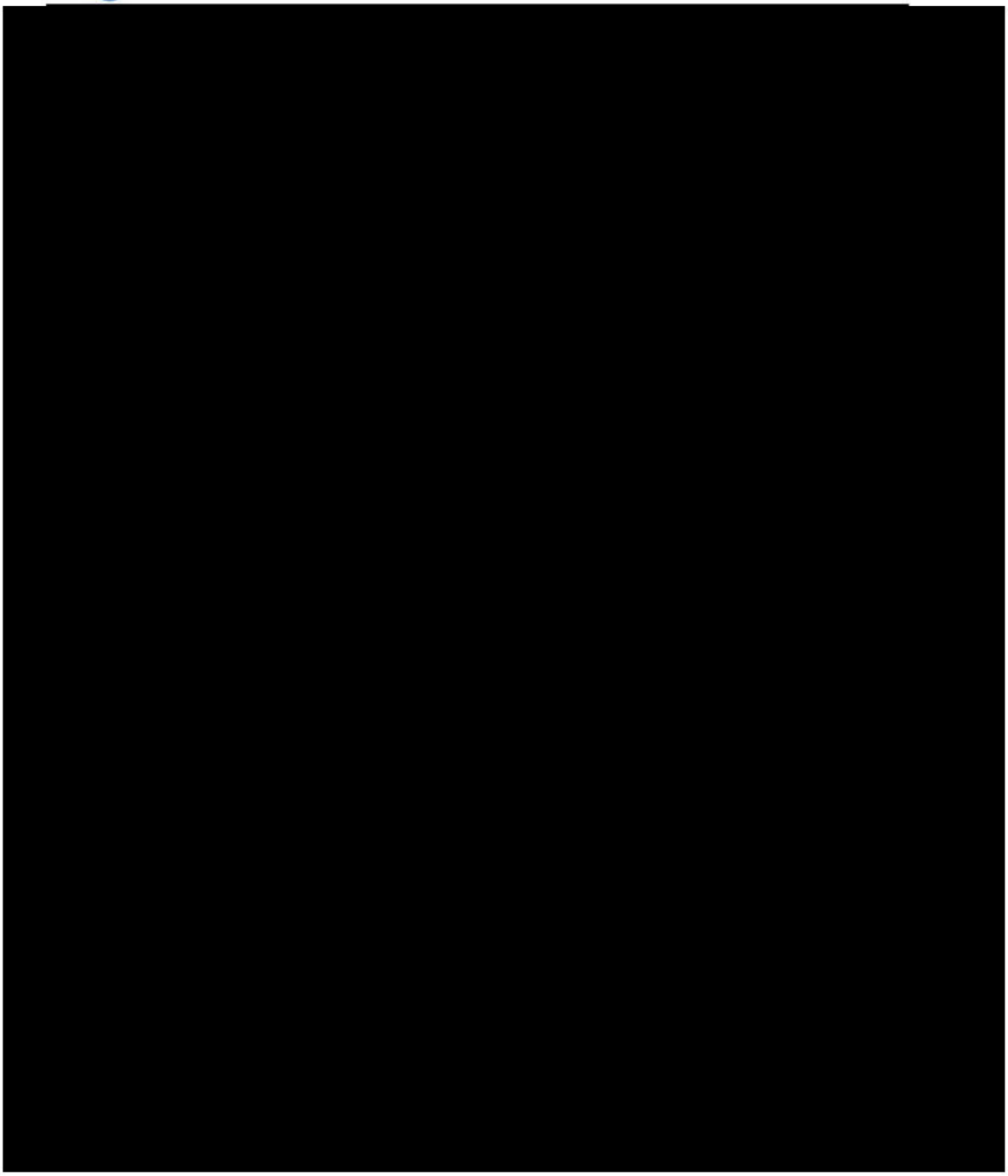

HITACHI GEH PROPRIETARY INFORMATION *Engineering Calculation Sheet*

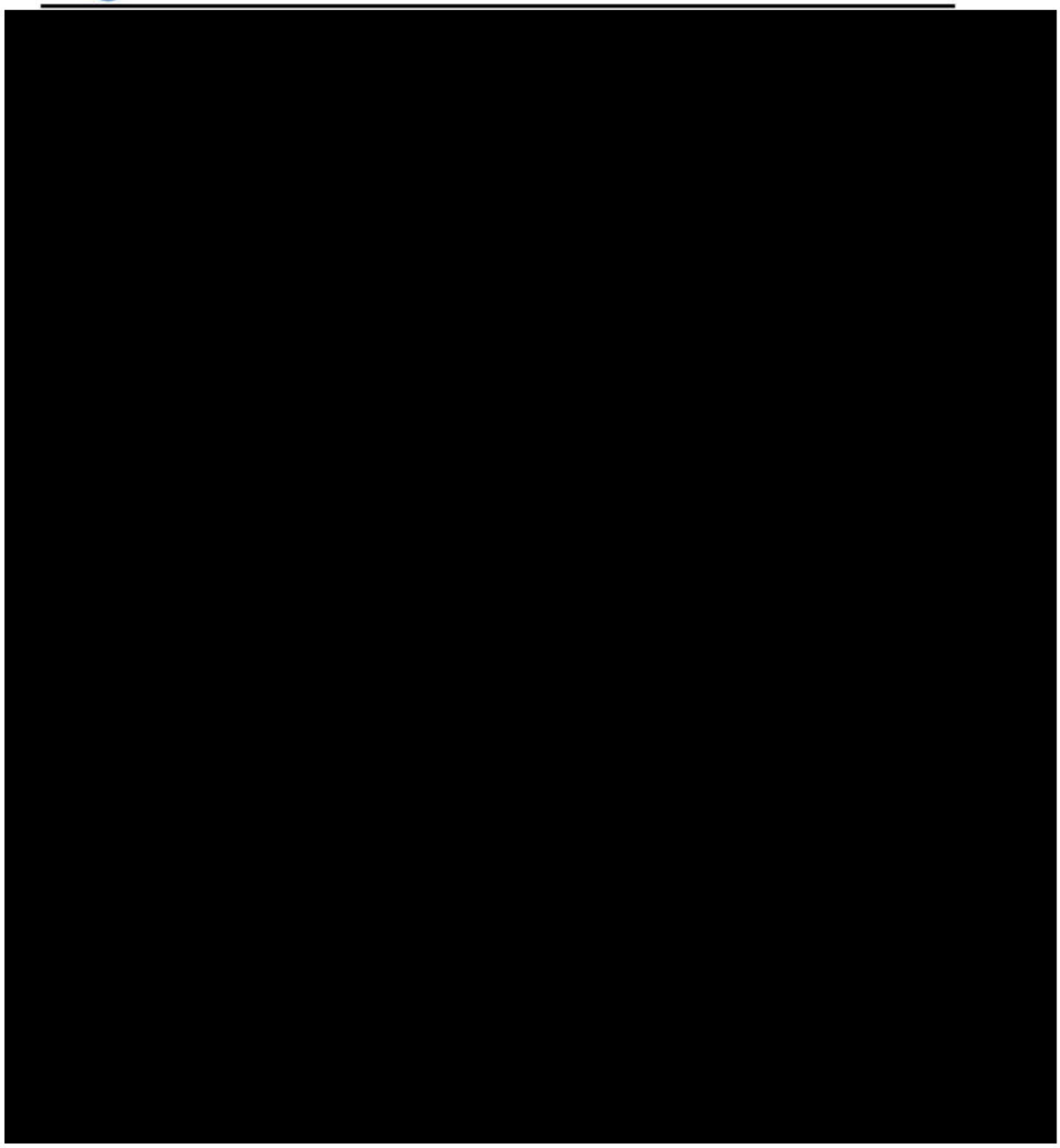

HITACHI GEH PROPRIETARY INFORMATION *Engineering Calculation Sheet*

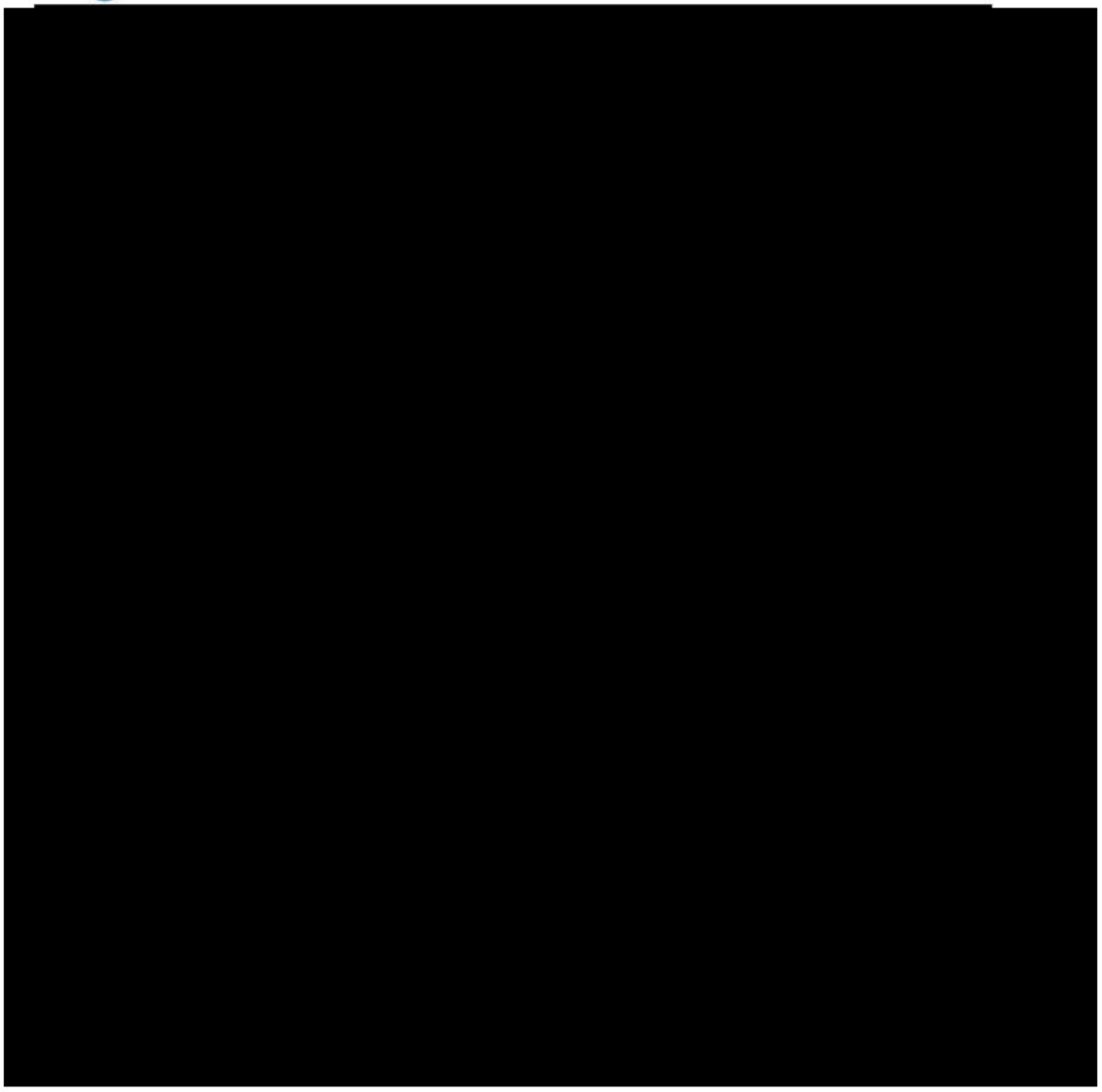

HITACHI GEH PROPRIETARY INFORMATION *Engineering Calculation Sheet*

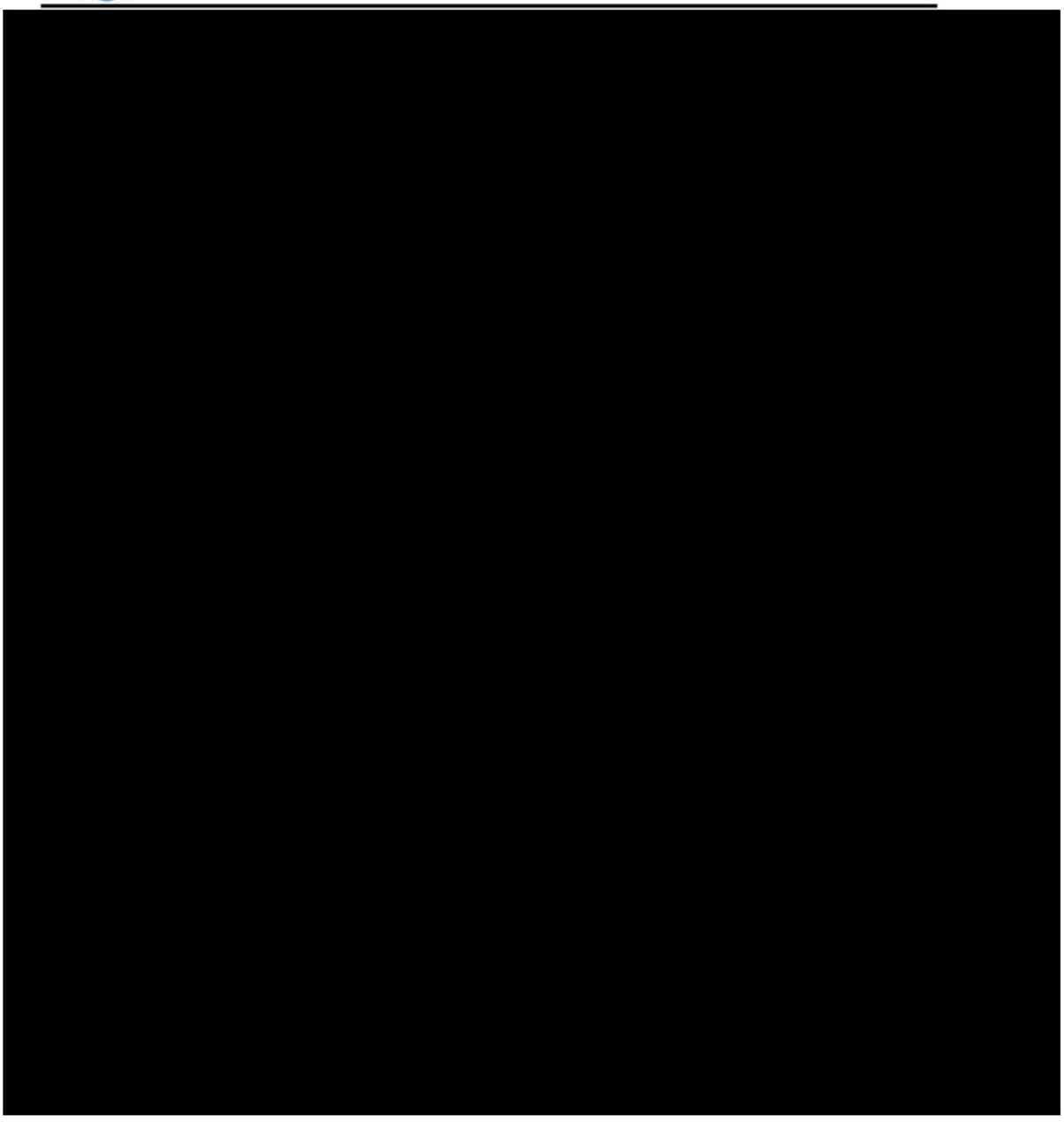

HITACHI GEH PROPRIETARY INFORMATION *Engineering Calculation Sheet*

A.17 RADIATION MONITOR LOCATIONS (REVISED)

A.17.1 INTRODUCTION

The ARM on the east wall (a portable detector) was moved to the west wall. This appendix is added to revise Figure 7-2, Radiation monitor locations, to reflect the current location of the Basin Pump Room radiation monitor.

A.17.2 FIGURE A.17, Radiation monitor locations (revised)

FIGURE A.17, Radiation monitor locations (revised)